Biomedical fibreoptic thermometer based on Cr^{3+}-doped crystal fluorescence – a feasibility study

Master's Thesis
by

Anna Ralsgård and Jenny Svensson

Lund Reports on Atomic Physics, LRAP-280
Lund, February 2002

Abstract

In this Master's Thesis a technique to optically measure the temperature is evaluated. The measurement is to be performed through optical fibres during photodynamic laser treatments of malignant tumours. For this technique Cr^{3+}-doped crystals were used. The lifetime and emission spectrum of the ions' fluorescence were measured, since the fluorescence is strongly temperature dependent. A piece of a crystal was attached to the tip of an optical fibre. The crystal was excited at 635 nm, which is the wavelength used for the treatment.

An accuracy in the temperature measurement of ± 0.3 °C was obtained for Cr:LiSAF in the region 20 – 70 °C. This is well below the requirements for this application. Alexandrite and Cr:YAG were also evaluated in this study, also yielding a very good accuracy. We found, however, that these crystals were not as good for this application as Cr:LiSAF because of other requirements. A laser treatment was simulated using pork chop as tissue phantom and the temperature was measured. The temperature was measured in three different ways, including the crystal fluorescence lifetime method. No significant increase in temperature could be seen after 15 minutes of illumination.

The technique to measure the temperature with optical fibres is to be incorporated in a complete system for interstitial photodynamic therapy. Before this is possible, further development is necessary.

Contents

1 Introduction

The aim of this Master's Thesis is to evaluate an optical technique to measure the temperature, during interstitial photodynamic therapy (IPDT) treatment of malignant tumours. During the treatment, fibres are inserted into the tumour. Laser light guided through these fibres induces, together with a certain compound, tumour cell death. If a local bleeding occurs close to the fibre tip, the temperature will increase due to the higher absorption of light in blood. The high absorption will reduce the efficiency of the treatment. Therefore, it would be favourable if the temperature could be monitored, so the treatment can be optimised and the outcome can be accurately predicted.

A way to solve this could be to use a crystal with a strong temperature dependent fluorescence. One would like to be able to use the fibres already inserted in the tissue for the temperature measurements. This can be done by attaching small pieces of the crystals to the fibre tips. Since the treatment wavelength is 635 nm, it would be preferable if the crystal can be excited at this wavelength. The crystal fluorescence should be temperature dependent between 20 – 70 °C, because these temperatures can be interesting in medical applications. Above 55 °C coagulation of proteins can occur. Since IPDT is not a thermally therapeutic treatment, temperatures above 70 °C should not be interesting. The accuracy required is approximately 1 °C.

In the near future a complete IPDT system will be developed, which can treat tumours but also record fluorescence spectra to monitor the treatment. The method to measure the temperature evaluated in this project is meant to be included in the system.

2 Theory

2.1 Fluorescence

When an atom or a molecule absorbs light it will be excited. After a while it will return to its ground state by emitting light or transferring its absorbed energy to other particles by collisions. If the emitted light has the same wavelength as the absorbed light, it is called resonance radiation. If a part of the absorbed energy is lost by internal conversion between different vibrational levels the emitted light will have a longer wavelength and is called fluorescence, see Figure 1.[1]

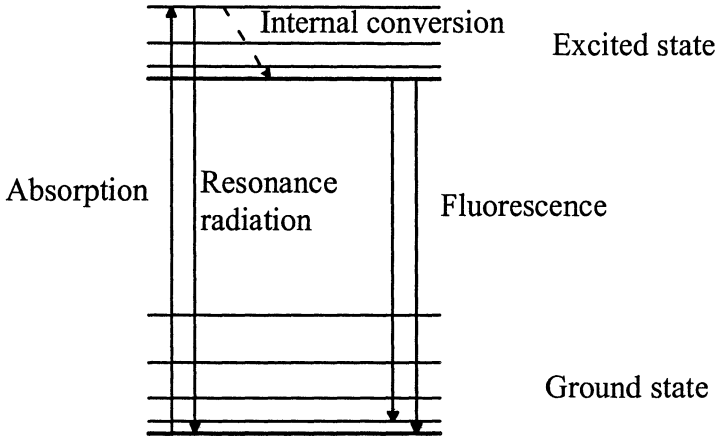

Figure 1. The principle of fluorescence

There is also another possible deexcitation path where the molecule can decay to a state with another multiplicity. This new state will have a longer lifetime than the originally excited state, because the transition to the ground state is spin-forbidden. The light emitted in the deexcitation to the ground state is called phosphorescence and is shown in Figure 2.[1]

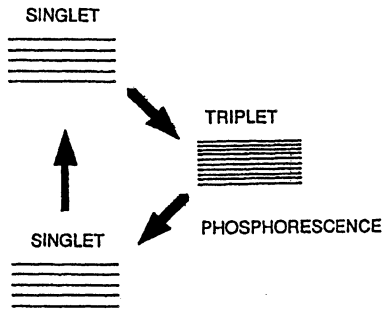

Figure 2. The principle of phosphorescence[1]

2.2 Interstitial photodynamic therapy

Photodynamic therapy, PDT, is a non-invasive method for treating locally situated tumours. The patient is given a photosensitising drug a few hours before the treatment. The photosensitiser can be given in three different ways of administration: orally, intravenously or as a cream on the skin. After a few hours the photosensitiser has selectively accumulated in the tumour and the treatment can begin. By illuminating the tumour through an optical fibre, with light of a wavelength matching an absorption peak of the photosensitiser, one can excite the photosensitiser. Because of a long lifetime in the excited state, the photosensitiser can interact with other molecules and an energy transfer is therefore possible. If the energy is transferred to an oxygen molecule, this molecule can be excited from a triplet ground state to a first singlet excited state, see Figure 3. This singlet state is very reactive and can oxidate proteins and nucleic acids, which can lead to cell death in the tumour. Direct cell death is the primary effect of the treatment, the secondary effects are for example inflammation and damages of the bloodvessels resulting in lack of oxygen. The secondary effects will also lead to cell death, but on a longer timescale, typically a few weeks.[2]

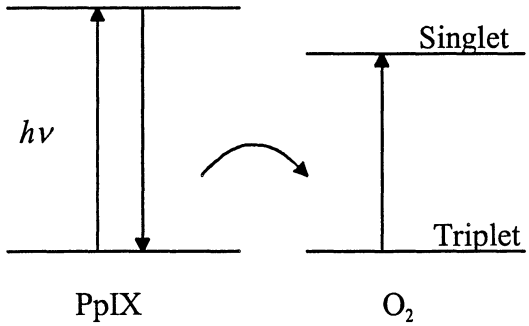

Figure 3. Energy transfer between a photosensitiser (PpIX) and oxygen

The main advantages with PDT are that the treatment is selective and that the treated areas heal fast. The procedure can be repeated and gives a good cosmetic result. A major disadvantage is that only superficial tumours can be treated and that the tumour thickness can only be a few millimetres to be treatable.[2] A solution to this problem is to use the invasive method interstitial photodynamic therapy, IPDT. The only difference between PDT and IPDT is that when using IPDT the light is guided directly into the tumour through optical fibres. This gives the opportunity to treat larger tumours and tumours deeply located. The use of more than one fibre makes it possible to measure the energy flux from the fibres, so that the energy dose can be monitored during the treatment.[3]

2.2.1 Autofluorescence

By illuminating human tissue with UV or near UV light, the tissue will emit fluorescence, called tissue autofluorescence, in the blue-green wavelength region. The fluorescence arises from different tissue fluorophores. The most important tissue fluorophores are tryptophan, collagen, elastin, nicotineamide adenine dinucleotide (NADH) and its phosphate NADPH. The fluorescence spectra for some of these fluorophores are seen in Figure 4.[4]

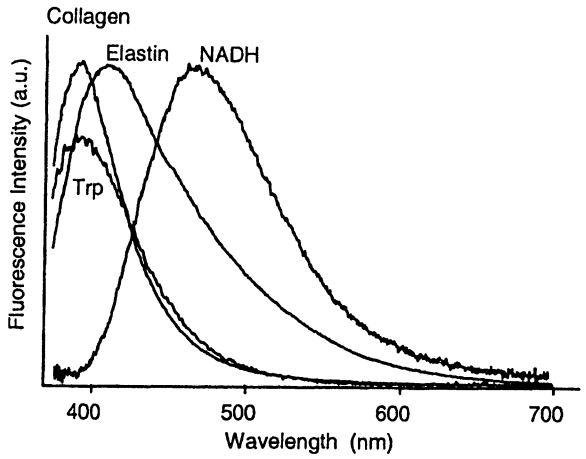

Figure 4. Fluorescence from some tissue fluorophores[4]

The fluorescence lifetimes of these fluorophores are in the nanosecond region. The autofluorescence in malignant tissue is lower than in normal tissue, due to the difference in the metabolism and in the amount of the different fluorophores.[2]

2.2.2 Photosensitisers

Compounds that accumulate in tumours to a higher degree than in normal tissue are called tumour selective agents. These compounds can be used to localise and characterise different diseases and also to treat tumours. When fluorescing tumour selective agents are used for diagnostics, the interesting area is illuminated with UV or blue light. The tumour markers absorb this light and after a while the absorbed energy is released as fluorescence light in the red region. During a PDT treatment the patient is given a tumour marker which in this case often is called a photosensitiser. Many of these photosensitisers have several absorption peaks in the region 400 - 780 nm. Due to the deeper penetration of the red light in the tissue, the absorption peaks in this region is used to allow treatment of larger tumour volumes. It is also possible to monitor the treatment because of the photosensitisers' ability to fluoresce.[2] Important properties of the photosensitisers are that they should have high selectivity in the tumours, have a fast clearence in the healthy tissue and should not be toxic.[5]

One photosensitiser is protoporphyrin IX, PpIX, but this is not the actual substance given to the patient during the PDT treatment, instead ALA, δ-aminolevulinic acid, is used. ALA is a substance that occurs naturally in the body and it participates in a biochemical process, the haemcycle. In the haemcycle ALA is transformed into the fluorescent and photodynamic PpIX. An Fe^{2+}-ion will then bind to PpIX and form haem. A specific enzyme, which is more produced in certain malignant cells, effects the haemcycle. This leads to an increased production of PpIX. When sufficient amount of haem is produced, the feedback between PpIX and haem decreases the haem production. This leads to a

higher accumulation of PpIX in these malignant cells. When using PpIX as a photosensitiser the treatment wavelength should be 635 nm, where PpIX has an absorption peak, see Figure 5.[2]

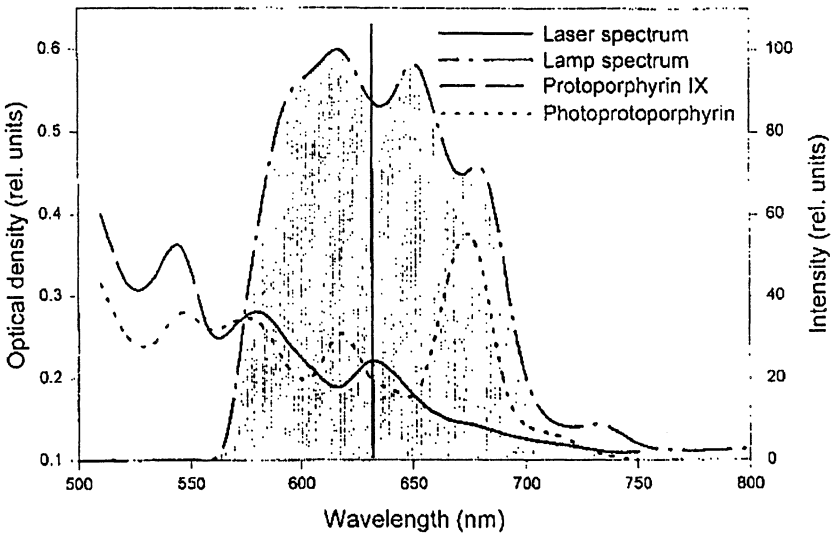

Figure 5. The absorption profile of PpIX[6]

To monitor the treatment, PpIX is excited with laser light at 405 nm and the fluorescence spectrum is studied. Typical spectrum can be seen in Figure 6 with fluorescence from PpIX, tissue and photoproducts. Photoproducts are generated when the photosensitiser is oxidised by the reactive singlet oxygen.[2] The fluorescence lifetime of PpIX is approximately 15 ns. Different components of the molecule have different lifetimes, therefore it is difficult to measure one specific lifetime for PpIX.[7]

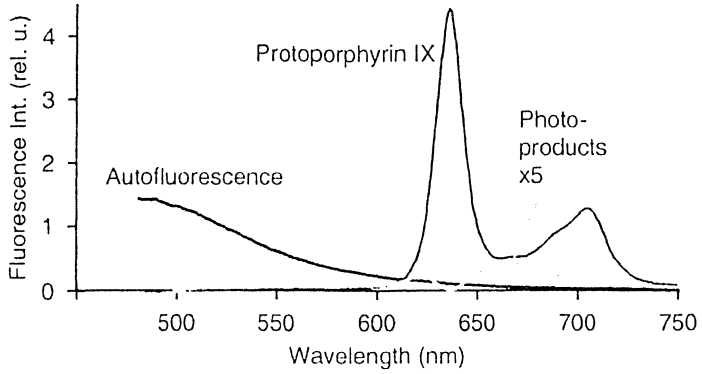

Figure 6. Spectra with fluorescence from the tissue, PpIX and photoproducts[2]

2.2.3 IPDT system

The medical group at the Division of Atomic Physics at Lund Institute of Technology has developed an IPDT system, which is described below.
The laser in the system is a continuous wave (CW) diode laser at 635 nm. The maximum output power from the laser is 2 W. The laser light is coupled into a fibre, which leads into a beamsplitting unit, see Figure 7.[3]

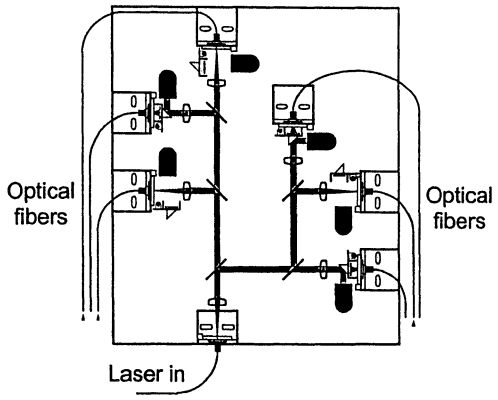

Figure 7. The beamsplitting unit of the developed IPDT system[3]

In the beamsplitting unit the light is divided and focused into six different fibres with a diameter of 400 μm. These fibres are then placed in the tumour for treatment. During the treatment it is possible to measure the light fluence rate at the individual fibre tip locations. If one or more of the fibres transmit laser light, the other fibres can be used to detect the light from the transmitting fibres. The light is detected with a photo diode placed in the beam path for the measuring fibres. This gives the opportunity to control the treatment and dosimetry.
A custom made program is used to control the beamsplitting unit and to measure the light fluence rate. The program is divided into two parts. The first one calculates the absorbed fluence rate in every part of the tissue for each fibre. The second part of the program guides the operator through the whole treatment. During the treatment, the theoretical absorbed dose is displayed to give the operator a feeling of what is happening.[3]

2.3 Optical measurements of the tissue temperature

The aim of our project is to find a way to measure the temperature in the tissue during an IPDT treatment. Preferably one would like to be able to measure the temperature with the same fibres that delivers the light during the treatment. A possible way to do this is to attach a crystal, whose fluorescence is temperature dependent, to the fibre tip. Some requirements are that it should be possible to excite the crystal at the treatment wavelength, 635 nm, and that the crystal's fluorescence should be sensitive to temperatures in the region 20 – 70 °C. An advantage would be if the fluorescence spectrum from the crystal easily could be seperated from tissue autofluorescence. It is also desirable that the crystal should not absorb light around 405 nm, to prevent interference with the PpIX fluorescence measurements during the IPDT treatment. A discussion of some possible crystals follows.

2.3.1 Rare-earth metals

Rare-earth dopants are incorporated into optical materials as trivalent ions, for which the number of 4f electrons increases from one in Ce^{3+} to 13 in Yb^{3+}. Most of the optical properties of rare-earth doped materials depend on the optical transitions between the 4f electronic levels of the rare-earth ions. The energies at which these transitions occur are only weakly effected by the host material because outer filled electron shells screen the 4f electrons.[8]

The screening of the 4f electrons also reduces broadening of the f-f transitions due to environmental effects and therefore the absorption and emission spectra of rare-earth doped materials are characterised by narrow line transitions. This would make it easy to detect the fluorescence from the crystal even if other fluorophores were present. One property of the rare-earth ions that is determined by the host material is the rate of nonradiative relaxation of the excited states of the ions. If the energy gap is large relative to the characteristic phonon energy of the host, the probability of nonradiative relaxation is low since it requires the emission of a large number of phonons. This process can proceed quite fast for closely spaced levels or high phonon energies. For certain ions/host combinations, the temperature dependence of multiphonon nonradiative relaxation can be quite pronounced, indicating that this effect can be used for temperature sensing. The equilibrium population distribution of the rare-earth energy levels changes with temperature. At zero temperature all rare-earth ions are in their ground state and the absorption spectrum is characterised only by transitions that originate from the ground state. When the temperature increases the width of the Boltzmann distribution increases and low lying energy levels will be populated. The absorption spectrum will then exhibit absorption lines that originate from these low-lying states. When the temperature increases even more, the strength of these absorption lines grows.[8]

In Figure 8 the energy levels of the rare-earth metals can be seen. After studying the energy levels no suitable transitions at 635 nm was found. Therefore the rare-earth metals did not seem to be the best choice for the project.

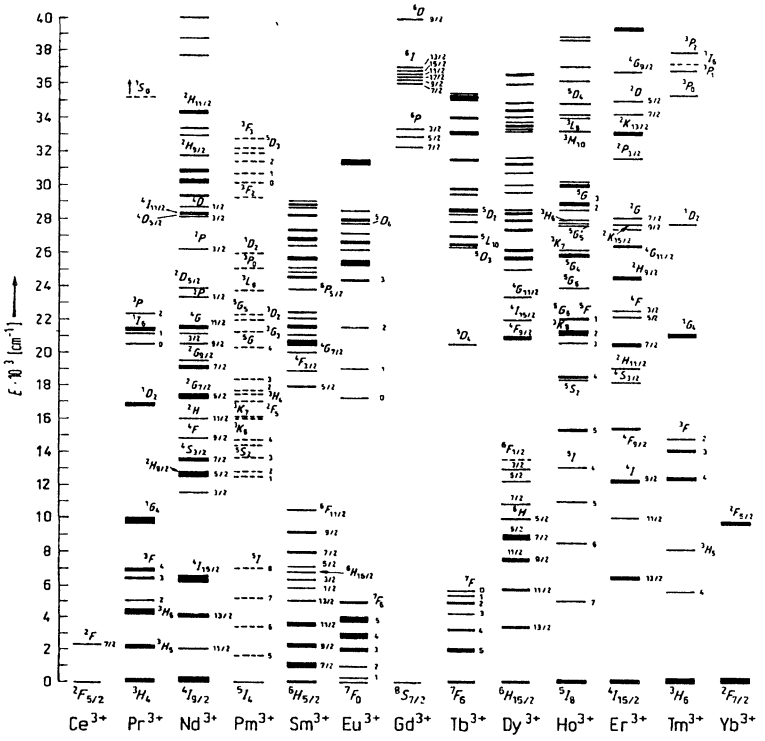

Figure 8. Energy levels of the rare-earth metals[9]

2.3.2 Cr^{3+}-doped materials

Cr^{3+}-ions in ionic crystals interact strongly with the crystal field and the lattice vibrations. The crystal field arises because of the influence on the Cr^{3+}-ion from the neighbouring ions. The interaction between the Cr^{3+}-ions and the crystal field arises due to the fact that there are no outer shells to shield the three valence electrons. As a result Cr^{3+}-activated materials are characterised by a wide absorption spectrum, from UV to infrared. This has two advantages, the possibility to choose excitation source and that a small drift in the excitation source will not cause a significant change in fluorescence intensity. Because of the strong crystal field interaction, the energy gaps of the electronic levels of Cr^{3+} can vary from one host crystal to another. The temperature dependence of the fluorescence lifetime varies with the energy gap and will thus differ for different Cr^{3+}-doped materials. To measure the temperature using the fluorescence signal from a Cr^{3+}-doped crystal, the crystal should be selected with respect to the temperature interval of interest.[10]

The crystal field strength will vary in different Cr^{3+}-doped materials, due to the lattice configuration in the different hosts. The hosts discussed will have an octahedral lattice configuration. The ground state in Cr^{3+} is always $^4A_2$, independent of the strength of the crystal field. The two excited energy levels involved, following excitation at 635 nm, are $^4T_2$ and ^2E. The energy splitting between these two low lying states is denoted:

$$\Delta E = E(^4T_2) - E(^2E).$$

ΔE varies strongly with the strength of the crystal field and can be both negative and positive. At high crystal field strength, for example in ruby and alexandrite, ΔE is positive and the emission of the Cr^{3+} is dominated by the transition, $^2E \rightarrow {}^4A_2$. In a low crystal field strength, for example in Cr:LiSAF, the dominating transition is $^4T_2 \rightarrow {}^4A_2$.[10] In

Figure 9 the energy for these two energy levels are shown for four different Cr^{3+}-doped materials. The crystal field strength is the energy difference between the two possible orbital levels for electrons in a Cr^{3+}-ion and is expressed as Dq. Where Dq depends on the distance between the ions in the lattice and the charge of the ions. The crystal field strength is often plotted as Dq/B, where B is a measure on the Coulomb interaction between the electrons.[11]

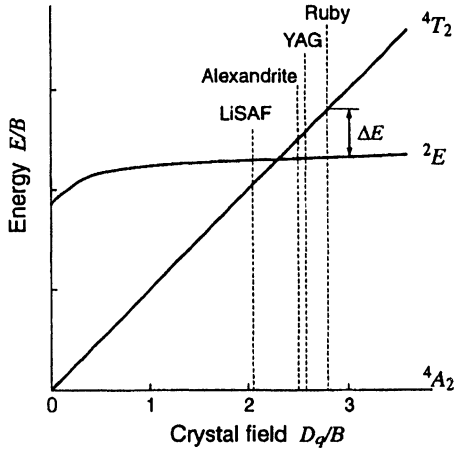

Figure 9. The electronic energy levels of the Cr^{3+}-ion in different host materials. The figure shows, E/B, the normalised energy of the low-lying excited states as a function of the normalised octahedral crystal field strength Dq/B[12]

In Figure 9 one can se that the energy difference between the ^2E state and the ground state $^4A_2$ is almost independent of the crystal field strength. This is due to that the electrons in these states occupy the same kind of orbitals, which are not directed towards other ions in the crystal. The energy difference between the ground state and the $^4T_2$ state depends on the crystal field strength, because of the change in electron orbitals between this state and the ground state. The electron orbitals in the $^4T_2$ state are directed towards neighbouring ions, which make the orbitals sensitive for changes in the crystal field. Due to the fact that different crystals have different crystal field strength, the energy difference between $^4A_2$ and $^4T_2$ will change.[11]

The emission spectrum of Cr^{3+} consists of two different features, a broad spectral band and two sharp peaks, so called R-lines. The broad band originates from the vibronic transitions, $^4T_2 \rightarrow {}^4A_2$, where ions in the $^4T_2$ state decay to the empty vibrational levels of the $^4A_2$ state. The R-lines appear because of the further split of the ^2E state into two levels, E and 2Ā, separated by a small energy gap. The R_1-line is the transition $E \rightarrow {}^4A_2$ and the R_2-line comes from the transition $2\bar{A} \rightarrow {}^4A_2$. The energy levels for a crystal with a high crystal field strength are seen in Figure 10.[10]

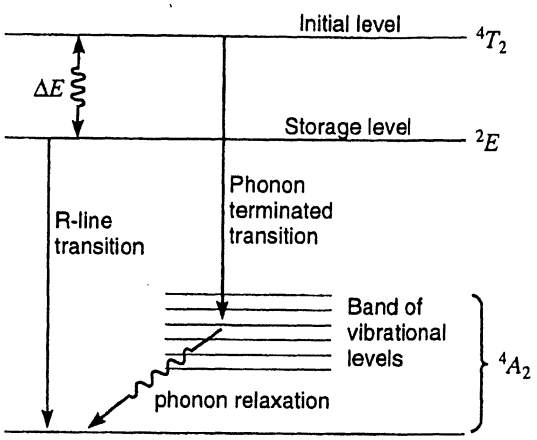

Figure 10. The energy levels for a crystal with a high crystal field strength[10]

Lattice vibrations interact with the electronic levels and transitions of the Cr^{3+}-ion through the modulation of the crystal field. The effects of this are the initiation of vibronic transitions, radiationless transitions and phonon scattering mechanisms. The first of these effects produces broad bands in the spectra, the second effect leads to a temperature dependent decrease of the fluorescence lifetimes of the R-lines and both the second and third effect can cause a thermal broadening of the R-lines.[13]

2.3.2.1 Low crystal field strength

In a low crystal field strength, the transition $^4T_2 \rightarrow {}^4A_2$ occurs through two processes, one is the radiative transition initiated from I seen in Figure 11. The other is a nonradiative process due to thermal quenching of the Cr^{3+}-ions. Some ions will be thermally elevated to Q, which is the energy crossing between the excited state and the ground state. These ions will decay to the ground state and will there undergo stepwise transitions to the lowest level of the ground state through nonradiative relaxation. These two processes compete with each other constantly.[10]

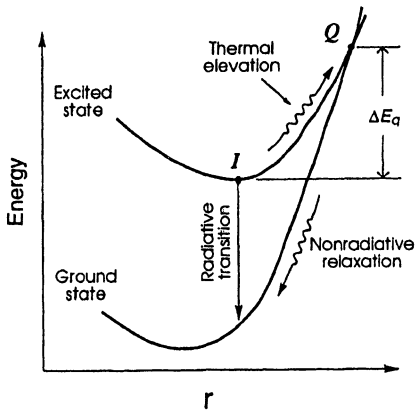

Figure 11. Energy levels as a function of nearest neighbour distance for crystals with a low crystal field strength[10]

When the temperature increases (above 275 K), more excited ions will be elevated to Q, due to the larger neighbour distance, and the nonradiative process, called quenching, will become stronger. Normally, the nonradiative transitions have a shorter lifetime and a decrease in the fluorescence lifetime is observed with increasing temperature. An

expression for the fluorescence lifetime, τ, for crystals with low field strength can be written as:

$$\tau = \frac{\tau_i}{1 + \beta e^{-\Delta E_q / kT}}$$

Where $1/\tau_i$ is the intrinsic radiative rate at the excited state, $1/\tau_q$ is the thermal quenching rate and $\beta = \tau_i/\tau_q$. ΔE_q is the energy difference between the bottom of the excited energy level and the energy level crossing Q, k is the Boltzmann constant and T is the temperature in Kelvin. The fluorescence intensity will decrease with increasing temperature due to the increase of nonradiative transitions.[10]

The impact of the ^2E state on the fluorescence lifetime is negligible. This is partly due to the low population of the ^2E state according to the Boltzmann distribution and partly due to that the transition $^2E \rightarrow {}^4A_2$ is forbidden both by parity and spin. The transition rate is thus one or two orders of magnitude lower than the transition $^4T_2 \rightarrow {}^4A_2$, and only a very small fraction of the excited ions will decay through this path. This explains why there are no visible R-lines in the emission spectra from Cr^{3+}-ions in crystals with low crystal field strength.[10]

2.3.2.2 High crystal field strength

In a high crystal field strength, the lowest excited state of the Cr^{3+}-ions is the ^2E state, see Figure 12. At low temperatures the emission is dominated by the transition $^2E \rightarrow {}^4A_2$ (R-lines), yielding an effective long fluorescence lifetime, since the transition is forbidden. The $^4T_2$ state has a shorter lifetime than the ^2E state. When the temperature increases a higher percentage of the Cr^{3+}-ions will populate the $^4T_2$ state according to the Boltzmann distribution. Consequently more ions will decay through the $^4T_2 \rightarrow {}^4A_2$ path, resulting in a decrease of the fluorescence lifetime. Thus at low temperatures the fluorescence properties are determined by the thermally activated populations of the ^2E and $^4T_2$ states. At high temperatures, above 600 K, more ions will be elevated to Q and nonradiative transitions become more significant and will speed up the decay even further.[10]

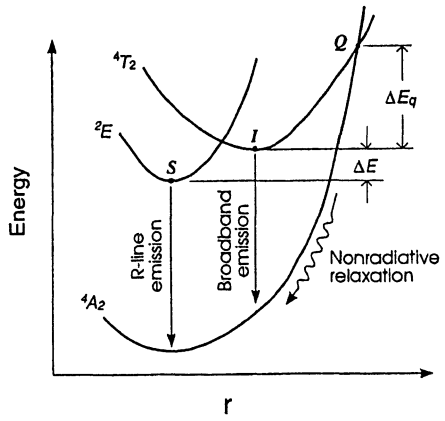

Figure 12. The energy levels as a function of nearest neighbour distance for a crystal with a high crystal field strength[10]

The fluorescence lifetime, τ, for crystals with a high crystal field strength, can be written as:

$$\tau = \tau_s \frac{1 + 3e^{-\Delta E / kT}}{1 + \alpha e^{-\Delta E / kT} + \beta e^{-(\Delta E_q + \Delta E)/kT}}$$

τ_s is the lifetime of the ^2E state, τ_i is the lifetime of the $^4T_2$ state and $1/\tau_q$ is the thermal quenching rate. $\alpha = \tau_s/\tau_i$ and $\beta = \tau_s/\tau_q$. ΔE is the energy gap between the ^2E and $^4T_2$ states, ΔE_q is the energy difference between the bottom of the excited energy level, $^4T_2$, and the energy level crossing Q, k is the Boltzmann constant and T is the temperature in Kelvin.[10]

2.3.3 Different Cr^{3+}-doped crystals

2.3.3.1 Alexandrite

Alexandrite is the gain medium used in a certain type of tunable solid-state lasers, the alexandrite laser. The peak emission wavelength of the alexandrite laser is 760 nm, with a bandwidth of 100 nm. The crystal is a $BeAl_2O_4$ in which Cr^{3+}-ions replace some of the Al^{3+}-ions.[14]

The two absorption bands of alexandrite, seen in Figure 13, are associated with the transitions $^4A_2 \rightarrow {}^4T_1$ and $^4A_2 \rightarrow {}^4T_2$. These transitions involve changes in the orbitals of the electrons and make the Cr^{3+}-ion very sensitive to the crystal field environment. Vibrational modulation of the crystal field strength produces the broad bands. There are three sets of sharp lines at 470 nm, 650 nm and 680 nm. These transitions involves spin-flips of the electron wave function without changing the orbitals of the electrons, thus they become insensitive to vibrational modulation of the crystal field and appears as sharp lines.[10]

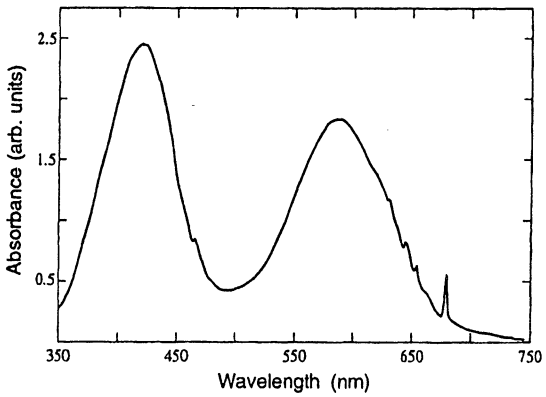

Figure 13. Absorption spectrum of alexandrite at room temperature[10]

The major features of the emission spectrum seen in Figure 14 are the two sharp lines, R_1 and R_2, and the broad vibrational band peaking at longer wavelengths.[10]

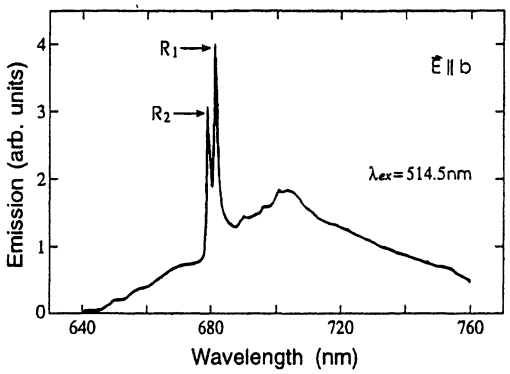

Figure 14. Fluorescence spectrum of alexandrite at room temperature[10]

2.3.3.2 Ruby

The ruby crystal consists of a natural crystal of Al_2O_3, in which some of the Al^{3+}-ions have been replaced by Cr^{3+}-ions. The more Cr^{3+}-ions there are in the crystal the redder the ruby gets. The ruby laser was the first operationable laser, built in 1960. Laser action usually occurs at 694,3 nm (R_1-line) but it can also lase at 692,8 nm (R_2-line).[14]
The absorption spectrum of ruby in the visible region consists of two broad bands centered at 400 nm and 550 nm, seen in Figure 15.

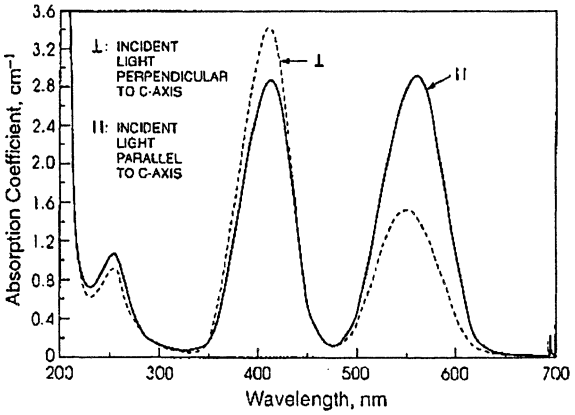

Figure 15. The absorption spectrum of ruby[10]

In Figure 16 the emission spectrum of ruby is seen.[10] The R-lines are not resolved in the figure.

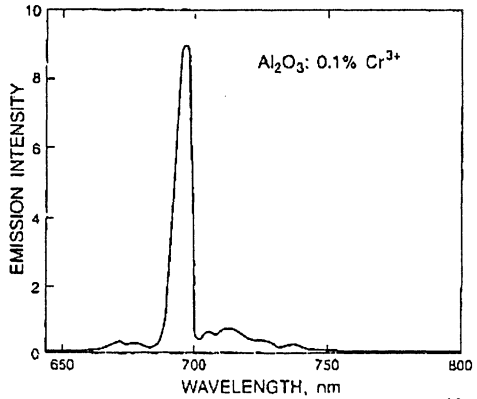

Figure 16. The emission spectrum of ruby[10]

2.3.3.3 Cr:YAG

The absorption spectrum of Cr^{3+}:YAG consists of two broad bands centered at 430 nm and 600 nm. The 600 nm band has a full width at half maximum of about 75 nm. The fluorescence spectrum shows two sharp emissions near 687 nm, the R-lines, and a continuum of fluorescence on both sides of the R-lines due to vibronic transitions.[15] In Figure 17 the fluorescence spectrum can be seen, but the two R-lines are not resolved.

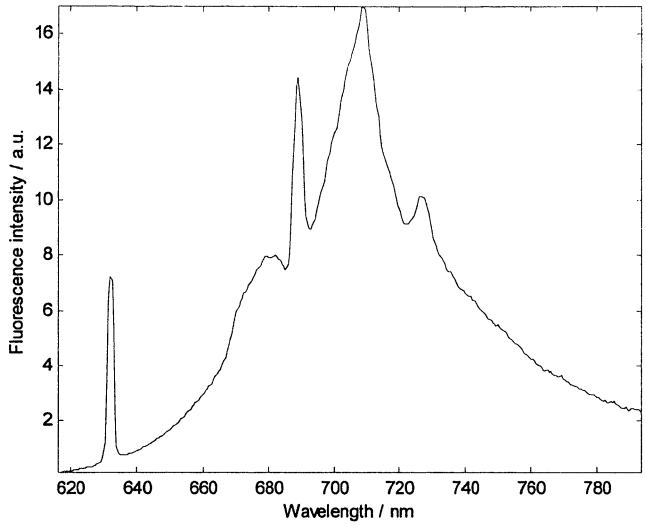

Figure 17. The fluorescence spectrum of Cr:YAG, where the crystal also is doped by 20 ppm of Co and 4 ppm Fe to suppress the strong red fluorescence. The excitation wavelength can be seen at 632 nm

2.3.3.4 Cr:LiSAF

A Cr:LiSAF crystal consists of a $LiSrAlF_6$ crystal, where some of the Al^{3+}-ions are replaced with Cr^{3+}-ions. Cr:LiSAF is used as a flashlamp, or a diode laser pumped source providing tunability around 850 nm. The large gain linewidth makes this medium attractive for generating femtosecond pulses.[14]

In the absorption spectrum of Cr:LiSAF illustrated in Figure 18, there are three broad bands. Parallel polarized light (π-light) at the top of the figure and perpendicular polarized light (σ-light) below.

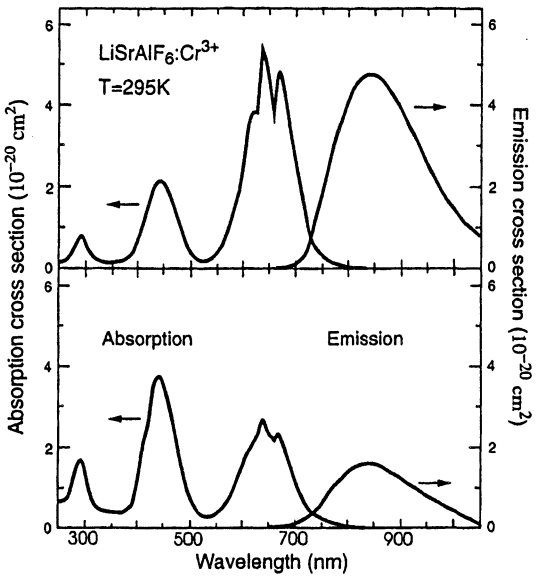

Figure 18. The absorption and emission spectra of Cr:LiSAF for π-light (upper part) and σ-light (lower part)[10]

The emission spectrum, also seen in Figure 18, spans the region from 700 nm to 1100 nm with the maximum intensity at about 825 nm. The broad band emission is due to the transition $^4T_2 \rightarrow {}^4A_2$.[10]

Cr:LiSAF fluorescence lifetime is comparatively short (~μs) to fluorescence lifetime of alexandrite and ruby (~ms).[16] This is because Cr:LiSAF is a crystal with low crystal field strength.

2.3.3.5 Temperature sensitivity

Different Cr^{3+}-doped crystals have different temperature dependence of the fluorescence. This leads to a higher sensitivity for temperature changes in some temperature regions than in others. In Figure 19 the temperature dependence on the fluorescence lifetime can be seen for alexandrite, Cr:LiSAF and ruby.[10]

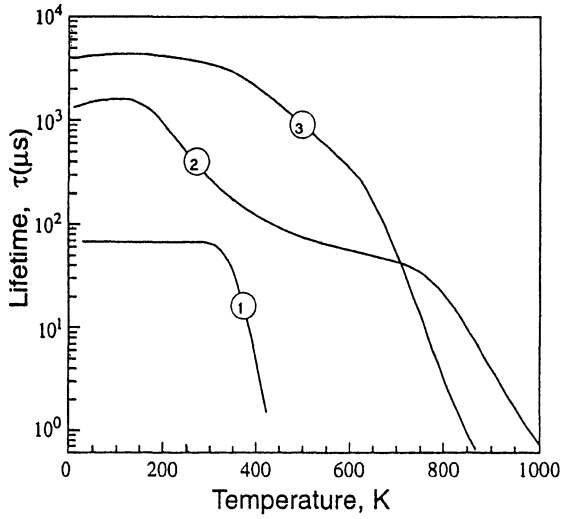

Figure 19. Temperature dependences of the fluorescence lifetime for Cr^{3+}-ions in different host materials; 1 LiSAF, 2 alexandrite and 3 ruby[10]

As can be seen in the figure, ruby has a very low sensitivity in the temperature region 300 – 400 K. Due to this, ruby was not an alternative for the project.

2.4 Two different methods to measure the temperature with fluorescence

When measuring the temperature, the fluorescence from certain crystals can be used in two different ways, fluorescence lifetime measurements and fluorescence intensity ratioing. Both these techniques are based on the thermalisation, which occurs between excited ionic energy levels, when the levels are populated using an excitation source. The two methods have the advantage of being independent of fluctuations of the excitation source.[17]

2.4.1 Fluorescence lifetime

The fluorescence lifetime can be measured by using an excitation source whose intensity is modulated by a sinusoidal signal, ν_m. The fluorescence signal will then be forced to follow the same modulation frequency as the excitation source, but lagging with a phase shift, illustrated in Figure 20.[10]

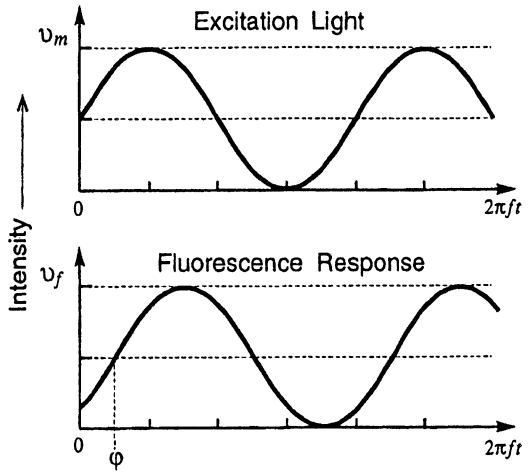

Figure 20. Phase measurement of fluorescence liftetime[10]

The fluorescence response signal is then given by

$$\nu_f = V_A \sin(\omega t - \varphi)$$

Where V_A is the amplitude of the fluorescence response signal, ω is the angular frequency of the modulation signal, t is the elapsed time and φ is the phase lag with respect to ν_m. The fluorescence lifetime, τ, is given by:[10, 18]

$$\tan\varphi = \omega\tau$$

2.4.2 Fluorescence intensity ratioing

The intensity ratio of the fluorescence, R, from two closely spaced levels in thermal equilibrium, seen in Figure 21, down to any other level is proportional to their population ratio determined by a Boltzmann term

$$R = \frac{I_2}{I_1} \propto e^{-\frac{\Delta E}{kT}}$$

Where I_1 and I_2 are the fluorescence intensities from level 1 and level 2, ΔE is the energy difference between the two levels, k is the Boltzmann constant and T is the temperature in Kelvin.[1]

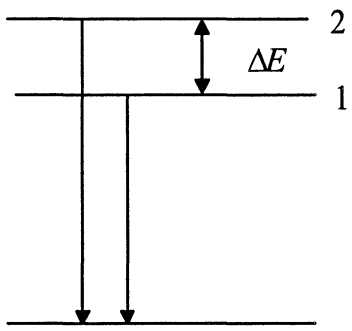

Figure 21. Two closely spaced levels in thermal equilibrium

3 Materials and methods

In the beginning measurements were performed on pieces of three different types of crystals. Two methods were tested; fluorescence lifetime measurements and fluorescence intensity ratioing. Two of the crystals were chosen for further experiments. The crystals were pulverised and attached to a fibre tip with glue. The one that gave the best result was used to make a calibration curve and to perform measurements on tissue phantom.

3.1 Initial experiments on three Cr^{3+}-doped crystals

Three different Cr^{3+}-doped crystals were found to be suitable for our purpose, namely alexandrite, Cr:YAG and Cr:LiSAF. These crystals have sufficient temperature sensitivity in the region 20 – 70 °C and can be excited by light at 635 nm. In Figure 22 the crystals are shown, also including a ruby crystal. No measurements were conducted with ruby, since it is known from literature to have low sensitivity in the selected temperature region.

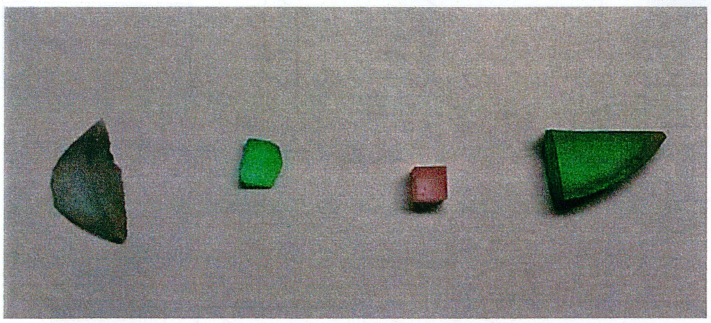

Figure 22. Picture of the crystals. From the left to the right, alexandrite, Cr:LiSAF, ruby and Cr:YAG

Both the intensity ratioing method and the fluorescence lifetime method were tested to evaluate which method gave the best accuracy.

3.1.1 Experimental set-up

The measurements were made with the set-up seen in Figure 23. The laser used was a He-Ne laser, Latronix, emitting light at 632.8 nm and with an output power of about 2.3 mW. The laser light was focused into an optical quartz fibre, with a diameter of 600 μm, from Fiberguide Industries, with the help of a lens, with the focal length of 50 mm and the diameter 25 mm. In the beam path there was a chopper wheel, model SR540 from Stanford Research Systems. The distal end of the fibre was led into an oven, model FN300, Nüve Microprocessor, where the fibre tip was in contact with the crystal. Here the laser light excited the crystal. A specially designed holder was placed in the oven. The holder was designed to fasten the crystal and to hold up to three fibres in their desired positions.

A detection fibre, fixed in the designed holder, see Figure 24, opposite to the fibre from the light source, collected both the fluorescence light from the crystal and some of the scattered laser light. This detection fibre guided the light to a photomultiplier tube, model R928 Hamamatsu. Between the fibre tip and the photomultiplier tube there was a holder

for optical filters. The holder has two different positions. In one position the filters only let the laser light pass and in the other position only the fluorescence light passes through. The signal from the photomultiplier tube was led to the input channel of a DSP lock-in amplifier, model SR830 from Standford Research Systems. The signal from the photomultiplier tube was a current and the lock-in amplifier measured the voltage that arised when the current passed through a resistance of 10 kΩ. A reference signal to the lock-in amplifier was obtained from the chopper wheel. The lock-in amplifier measured the phase difference between the input signal and the reference signal.

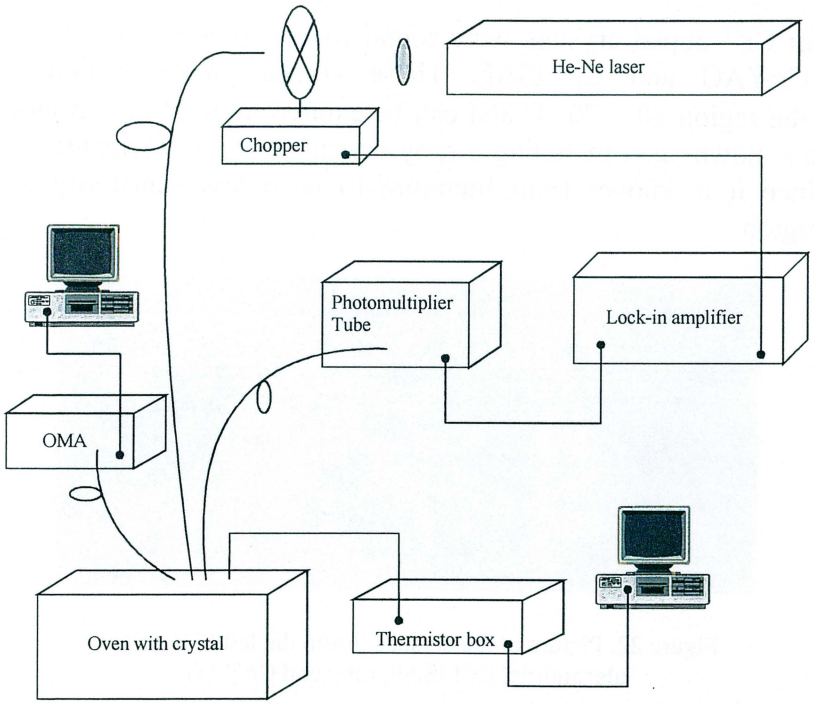

Figure 23. The set-up used to measure the temperature with crystals

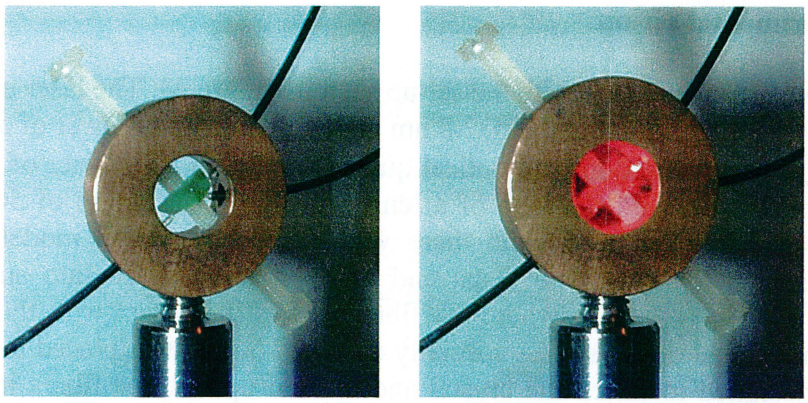

Figure 24. Pictures of the crystal in the holder with the three fibres, to the left the crystal with the laser off and to the right with the laser on

Another fibre guided some of the light emitted by the crystal to an optical multichannel analyzer system, OMA system, developed by the medical group at the Division of Atomic Physics at Lund Institute of Technology. A lay-out of the system is illustrated in Figure 25. The fibre collects fluorescence light as well as some of the excitation light. Some optical filters have to be used, to avoid saturation of the detector.
The OMA system can be used as a detector with the possibility to use an external or an internal light source. The internal light source is a pulsed nitrogen laser at 337 nm. The laser can also pump a dye laser to generate laser light at 405 nm. The laser light is guided to the sample through a fibre with a diameter of 600 μm, and the fluorescence is detected through the same fibre.

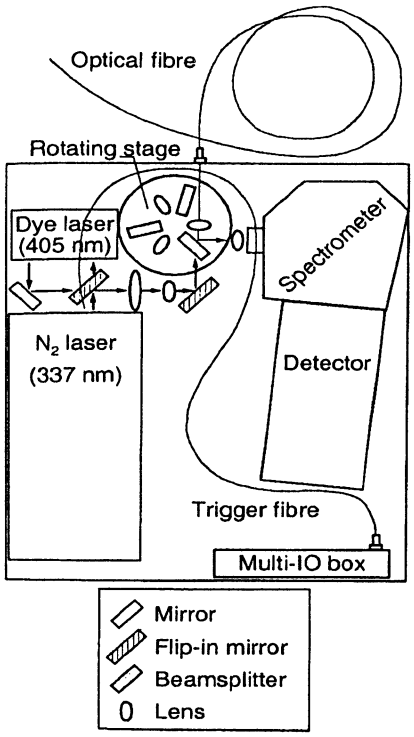

Figure 25. Schematic illustration of the OMA system[19]

In some of our experiments it was only the detection of the fluorescence light from the crystal that was interesting. In these experiments the laser light generated in the OMA system had to be blocked. The fluorescence was focused onto a spectrometer with the help of beam splitters, filters and lenses. The light was detected using an intensified CCD camera having 1024x128 pixels. The camera is thermo-electrically cooled. The obtained spectrum was time-integrated. This means that the CCD camera detected the light during a sufficiently long period of time to allow all fluorescence to be detected. A program written in LabVIEW controls the OMA system. Recorded spectra are shown on the computer screen.[19]

Two thermistors were used inside the oven to monitor the temperature changes. The temperature dependent parameter in a thermistor is the resistance of a semiconductor material. The resistance depends inversely on the number of mobile charge carriers. The number of charge carriers in a semiconductor is strongly dependent on the temperature. The number is proportional to $e^{-E/kT}$, where E is the energy gap, k the Boltzmann constant and T the absolute temperature. Typical change in the resistance is 4% per degree

Celsius. The thermistor is connected to an electric circuit, to measure its resistance.[20] The signal from the thermistors is analysed by a computer program, which makes it possible to monitor the temperature on a computer screen.

3.1.2 Adjustments

To get a good accuracy in the measurement of the fluorescence lifetime, the chopper frequency, f, should be chosen as

$$f \sim \frac{1}{2\pi\tau}$$

according to the chopper manual.

In Table 1 the optical filters used in the measurements of the various crystals are shown. The third and fourth columns show the optical filters used in front of the photomultiplier tube to let either the scattered laser light or the fluorescence through. The last column shows the chopper frequency. All coloured glas filters are from Schott.

Table 1. Optical filters

Crystal	**OMA system**	**Laser light**	**Fluorescence**	**Frequency**
Alexandrite	RG645 3 mm	ESCO 630 5BCP 5 mm RG645 4 mm	RG665 6 mm NG3 2 mm	465 Hz
Cr:YAG	-	ESCO 630 5BCP 5 mm RG645 1 mm NG11 1 mm NG5 2 mm	RG665 6 mm NG5 2 mm NG3 2 mm	78 Hz
Cr:LiSAF	RG645 1 mm RG665 1 mm	ESCO 630 5BCP 5 mm RG665 3 mm NG5 2 mm	RG695 3 mm RG665 3 mm NG5 2 mm	1955 Hz

Adjustments for the lock-in amplifier used in the experiments were:
Time constant: 1 x 1 s, 24 dB
Signal input: Couple AC, Ground
Reserve: Normal
Filters: Line
Reference: Pos Edge

Adjustments for the OMA system used in most experiments were:
Mode: 2
Gain: 1
20 shots per acqusition
Cooling: 1 °C

3.1.3 Description of the experiment

The crystal was put in the holder, which was placed inside the oven. The fibre with the excitation light, the dectection fibre to the OMA system and the detection fibre to the photomultiplier tube were put down inside the oven through a hole. The fibres were placed in the holder.
Two thermistors were placed in contact with the crystal. The laser was started and the oven was heated to the desired temperature. The temperature was monitored on the computer screen and when it had stabilized a measurement was made. First a fluorescence spectrum was taken with the OMA system. Then the filters in the photomultiplier tube were placed so only the fluorescence light was detected and the phase difference between the fluorescence signal and the reference signal was displayed on the lock-in amplifier. Then the filters were shifted so that only the laser light could be detected, and the phase difference between the laser signal and the reference signal was displayed. After this the temperature was raised to the next temperature and the procedure was repeated. Measurements were performed until temperatures of about 70 °C were reached. The data recorded at each temperature were the fluorescence spectrum, the two phase differences, the both thermistors' temperatures and the chopper frequency. Four separate series of measurements were made for each crystal, to study the reproducibility.

3.1.4 Calculations

To calculate the fluorescence lifetime, a program in MATLAB was written for each crystal. The two phase differences, the frequency and the temperatures from the thermistors were the input data to the program. The first computation was to calculate the phase difference between the fluorescence and the laser light, with the formula:

$$\Delta\varphi = \varphi_{fluorescence} - \varphi_{laser}$$

The lifetime could then be calculated as:[10]

$$\tau = \frac{\tan\Delta\varphi}{2\pi f}$$

A graph was drawn with the lifetime as a function of temperature for each measurement. The temperature was chosen as a mean value of the two thermistors' temperatures. A new graph was drawn where a polynomial of degree two ($ax^2 + bx + c$) was fitted to the data from the four measurements, with the least squares method. The standard deviation was calculated for the difference between the data points and the fitted curve. The standard deviation was also drawn in the graph. The relative standard deviation was calculated as the standard devation divided by the mean value of the lifetime.

In the fluorescence intensity ratioing method the ratio between the integrated intensity of the R-lines and the integrated intensity of a part of the vibrational band was calculated. The selected wavelength intervals for the R-lines (region 1) and for the vibrational band (region 2) can be seen in Figure 26, respectively. Region 2 was selected as a part of the vibrational band. A larger region could have been selected, but since Cr:YAG was doped by two other materials, a region not so close to the R-lines was chosen, to prevent disturbance from the two materials. Similar areas were chosen for the crystals. Since the

R-lines in Cr:LiSAF were not visible, the ratio was only calculated for alexandrite and Cr:YAG. The ratios were then plotted as a function of the temperature.

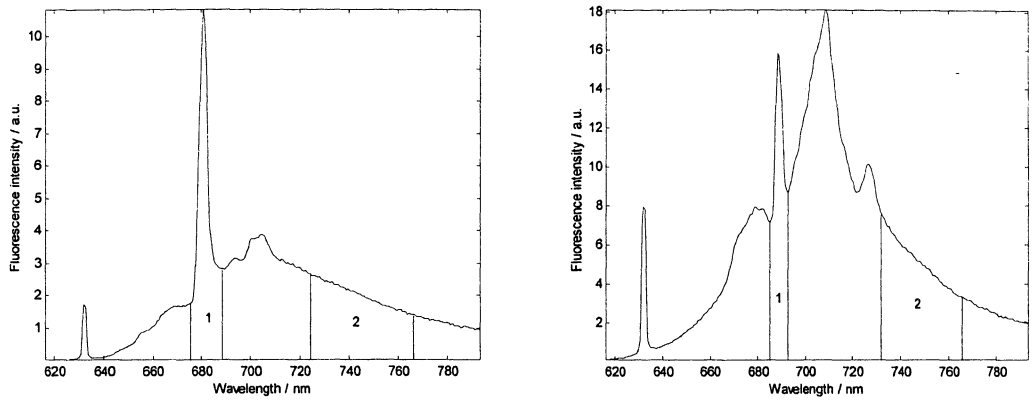

Figure 26. Selected wavelength intervals for the intensity ratioing method, alexandrite to the left and Cr:YAG to the right

3.2 Measurements on crystal attached to fibre tip

After the initial experiments alexandrite and Cr:LiSAF were chosen for the continuing experiments. The fluorescence lifetime method seemed to be more accurate than the fluorescence intensity ratioing method, so the lifetime method was chosen for the further experiments.

3.2.1 Attaching crystal to fibre tip

The crystals were pulverised in a mortar. One grain of the crystal was glued to the fibre tip. After curing, a second layer of glue was put around the crystal to minimise the influence of the environment on the crystal's fluorescence. Two different glues were evaluated to see if the glue effected the fluorescence. One of the glues, Norland Optical Adhesive 68, Norland Products, needed to be cured in UV-light for approximately ten minutes. The other glue used was an epoxy glue, Araldit Rapid, Casco, which needed to cure for several hours.

3.2.2 Experimental set-up

The experimental set-up was almost the same as in the previous section 3.1.1. The difference was that the crystal was much smaller and glued onto the tip of the fibre, coming from the laser. The fibre used was 400 μm in diameter. Since the laser emitted light at several wavelengths, a bandpass filter, 630 ± 5 nm, was placed in front of the laser.

3.2.3 Adjustments

In Table 2 the optical filters used for the experiment is shown. The third and fourth columns show the optical filters used in front of the photomultiplier tube to let either the laser light or the fluorescence through. The last column shows the chopper frequency. All coloured glas filter used are from Schott.

Table 2. Optical filters

Crystal	OMA system	Laser light	Fluorescence	Frequency
Alexandrite	RG645 3 mm RG665 1 mm	ESCO 630 5BCP 5 mm RG645 3 mm NG5 2 mm	RG645 3 mm RG665 1 mm	465 Hz
Cr:LiSAF	RG645 3 mm RG665 1 mm	ESCO 630 5BCP 5 mm RG645 3 mm NG5 2 mm	RG665 6 mm NG11 1 mm	1926 Hz

3.2.4 Description of the experiment

The fibres were put down into the oven and fastened in the holder and the thermistors were placed as close to the small crystal as possible. The experiment was conducted in the same way as in section 3.1.3, with the exception that only a few measurements were done with the OMA system, to study the two types of glue used, and only two measurement series for each crystal were performed. Calculations were conducted in the same way as in section 3.1.4.

3.3 Fibre measurements with PDT laser

After selecting the best suited crystal for our purpose, Cr:LiSAF, the fibre was tested with a more powerful laser, a PDT laser. A new fibre had to be made since the first one was broken. Another difference was that both the excitation light and the fluorescence light were guided through the same fibre. With this new set-up a calibration curve was made.

3.3.1 Experimental set-up

The experiment was performed with the set-up seen in Figure 27. The laser was a Ceralas™ PDT635, CeramOptec, diode laser. Since the laser spectrum had a continuum from 630 - 700 nm with a peak at 635 nm, a bandpass filter 635 ± 5 nm was inserted in front of the laser, so that no laser light, except 635 nm, could influence the fluorescence measurements. The laser was focused into the fibre with a lens system, which produced a 1:1 image of the object.

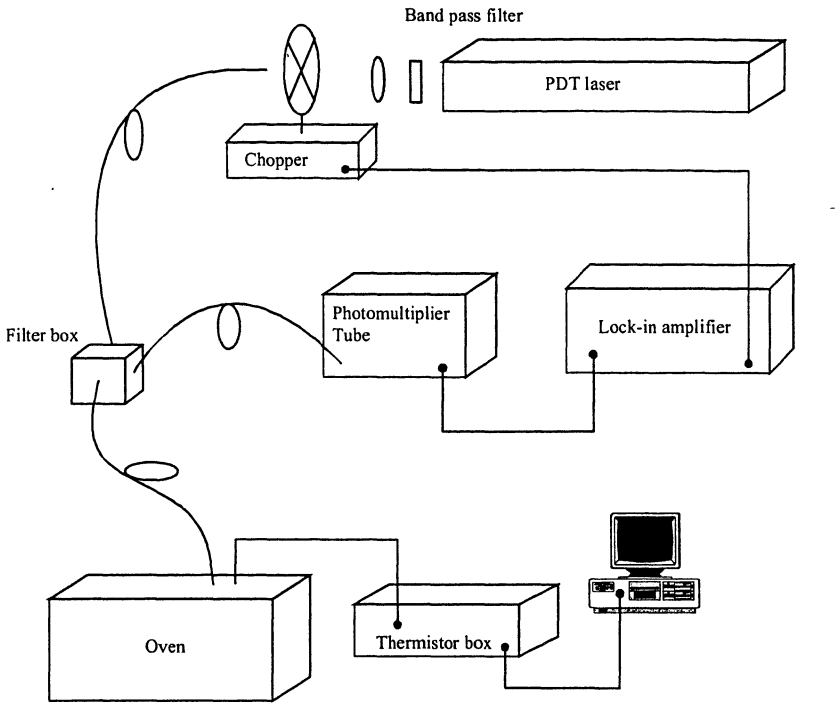

Figure 27. The experimental set-up to make the calibration curve

To be able to excite the crystal and detect the fluorescence light through the same fibre, a small box containing a beamsplitter (50/50) and three fibre connections was used. The box can be seen in Figure 28.

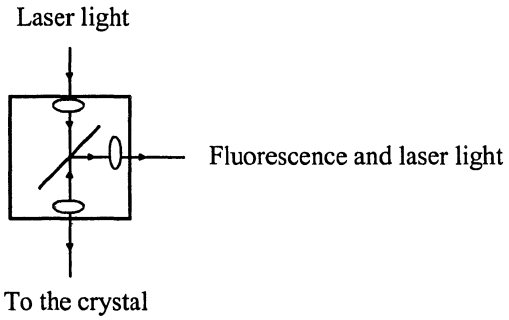

Figure 28. The filter box

From one of the connections the laser light is partly transmitted straight through the box into the opposite fibre, which leads to the crystal. The fluorescence light from the crystal enters the box and is partly reflected at the beamsplitter into the third fibre, which leads to the photomultiplier tube.

3.3.2 Adjustments

In Table 3 the optical filters used for the experiment is shown. The columns in the middle show the optical filters used in front of the photomultiplier tube to let either the laser light or the fluorescence through. The last column shows the chopper frequency. All coloured glas filters are from Schott.

Table 3. Optical filters

Crystal	Laser light	Fluorescence	Frequency
Cr:LiSAF	ESCO 630 5BCP 5 mm RG645 3 mm RG665 3 mm	RG695 3 mm RG715 3 mm RG645 3 mm NG4 2 mm	1950 Hz

Adjustments for the OMA system used in the experiment were:
Mode: 2
Gain: 6
400 shots per acqusition
Cooling: 1 °C

3.3.3 Description of the experiment

The lifetime was measured for several temperatures in the same way as in previous experiments, see section 3.1.3. The laser power was set to 1.9 W, but only about 7 mW came out of the fibre with the crystal, as the set-up could not be optimised for high output. After three series of measurements a calibration curve for the fibre was made. The calculations were conducted in the same way as in section 3.1.4.

Some spectra were taken with the OMA system, to study the fluorescence from Cr:LiSAF and tissue. The crystal and tissue were excited at 405 nm. One spectrum was recorded from a piece of Cr:LiSAF and one was recorded with the fibre in contact with the skin. A spectrum was also recorded from the skin with the fibre that had a piece of crystal glued to the tip.

3.4 Test measurements on pork chop

To see if it was possible to measure the temperature with the same accuracy in tissue as in air with the equipment, an experiment was made on pork chop as a tissue phantom.

3.4.1 Experimental set-up

The set-up is seen in Figure 29 and the adjustments were the same as in section 3.3.2. The fibre tip with the crystal was now placed between two pork chops inside the oven. The thermistors were placed on either side of the fibre, thermistor 1 placed 1 – 2 mm from the fibre and thermistor 2, 5 - 6 mm from the fibre. A compact fibre-optic fluorosensor using a CW diode laser, emitting at 396 nm, was now used to measure the fluorescence emission spectrum. The spectrometer in the fluorosensor was an Ocean Optics S2000.[21]

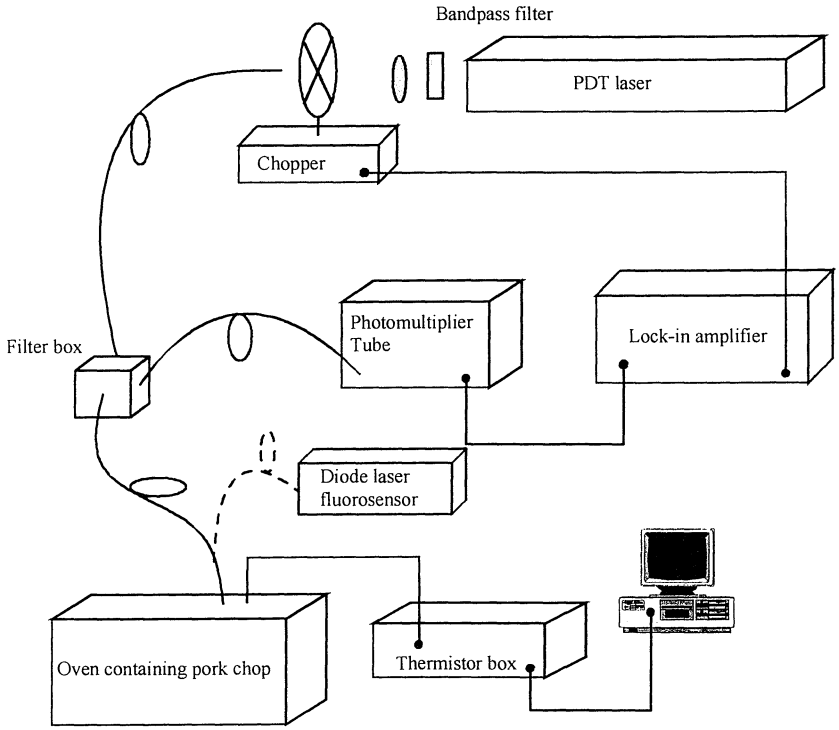

Figure 29. The experimental set-up for measurements on pork chop

3.4.2 The experiment

The temperature in the oven was raised and when the temperatures, measured by the thermistors, had stabilized a fluorescence lifetime measurement was performed in the same way as in section 3.1.3. A spectrum with the laser diode fluorosensor was also recorded. This was repeated until the pork chop reached the temperature 59 °C. After the measurements were performed, a photo was taken of the crystal on the fibre tip when it was placed on the pork chop. This can be seen in Figure 30.

Figure 30. The placement of the fibre with crystal and the thermistors on the pork chop

The lifetime was calculated for the different temperatures and was drawn in the same figure as the calibration curve. The lifetime was plotted as a function of temperature of the closest thermistor (thermistor 1).

3.5 Simulation of an IPDT treatment

The final step was to simulate an IPDT treatment. This was done by placing the fibre, with the crystal, between two pork chops and illuminating the tissue for 15 minutes, through the fibre. To overview the temperature distribution after the 15 minutes of illumination an IR camera was used. To get a uniform temperature distribution in the pork chops before the experiment, they were placed in room temperature for one day. A more natural situation would be if the pork chops had had a temperature of approximately 37 °C, like tissue during a real IPDT treatment. With our equipment it would be too difficult to achieve a uniform distribution at this temperature.

3.5.1 Experimental set-up

The set-up can be seen in Figure 31. The adjustments were the same as in section 3.3.2. The IR camera used was an uncooled, AGEMA 570 Elite, Flir Systems Inc. The power of the laser was set to 1.9 W. When the measurements were conducted the fibres were in position 1 and the power out from the fibre with the crystal was about 7 mW. During the treatment the fibres were in position 2, where the fibre from the laser was connected directly to the fibre with the crystal. The output power from the fibre with the crystal was now about 37 mW. The output powers were measured with a power meter, NOVA PD300, Ophir. The fibre was placed in position 2 during the treatment to maximise the power, to see if there was any increase in the temperature in the tissue.

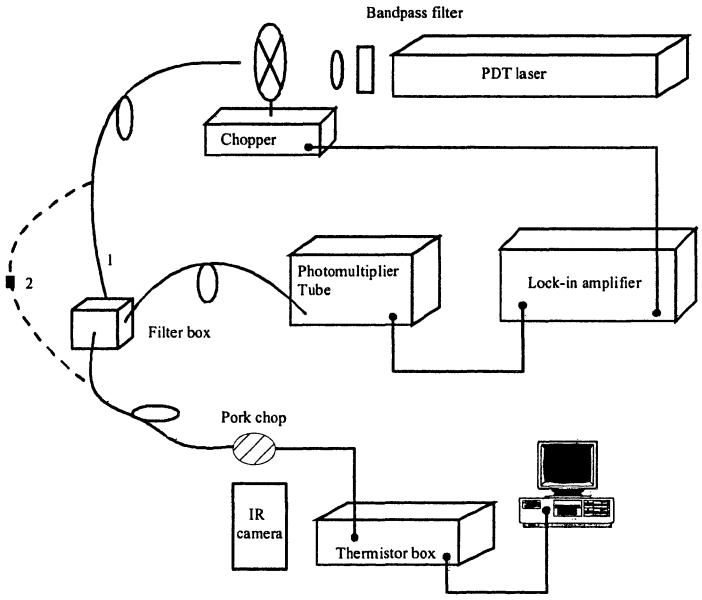

Figure 31. Experimental set-up for the simulation of an IPDT treatment

3.5.2 Description of the experiment

The laser was turned on with the fibre in position 1 and before the fibre was placed in position 2, a picture was taken with the IR camera. The phase differences for the exciting light and the fluorescence light were measured. After subsequent 15 minutes of illumination with the fibre in position 2, the fibre was again placed in position 1 and the phase differences were measured. A new picture was also taken with the IR camera to measure the temperature distribution.

4 Results

4.1 Initial experiments on three Cr^{3+}-doped crystals

As mentioned above three different crystals were evaluated; alexandrite, Cr:YAG and Cr:LiSAF. Two methods based on fluorescence lifetime and fluorescence intensity ratioing were tested. The reproducibility and temperature sensitivity for each crystal were investigated.

4.1.1 Alexandrite

In Figure 32 the lifetime for alexandrite is seen as a function of temperature. Four different series of measurements are included and the graph shows a good reproducibility.

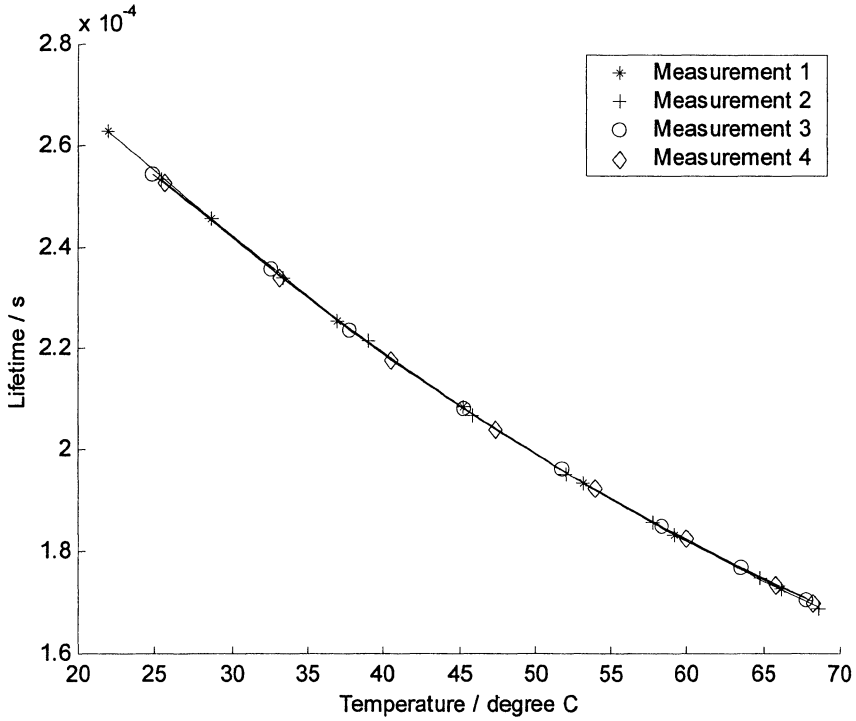

Figure 32. The lifetime as a function of temperature for alexandrite, almost a perfect overlap of the curves indicates a good reproducibility

The curve fitted to the four measurements and the standard deviation are included in Figure 33. The standard deviation was determined to 2.5 x 10^{-7} s and the relative standard deviation was 0.12 %. Only a fraction of the curve is shown in the graph. Taking one specific lifetime and estimating the temperature interval between the limits of the standard deviation for this lifetime makes an estimation of the sensitivity. The temperature sensitivity for alexandrite is estimated to ± 0.2 °C in the studied interval.

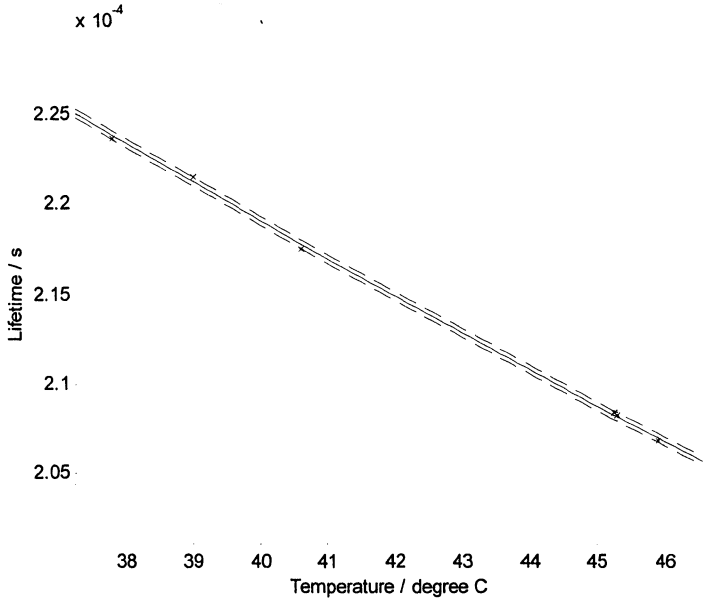

Figure 33. The fitted curve to the four measurements for alexandrite, solid line, and the standard deviation, dashed line

Figure 34 illustrates the results from the fluorescence intensity ratioing method for the four measurements that were conducted for alexandrite. The reproducibility again indicated by the figure. The reproducibility is obviously not as good as for the fluorescence lifetime method.

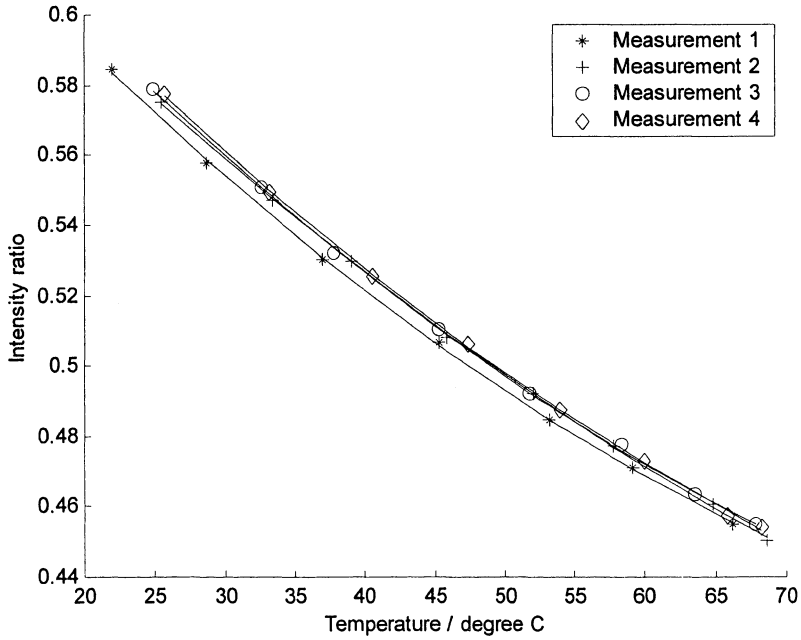

Figure 34. Fluorescence intensity ratio as a function of temperature for alexandrite

4.1.2 Cr:YAG

The lifetime for Cr:YAG as a function of temperature is seen in Figure 35. Four different measurements are included and the graph shows a good reproducibility.

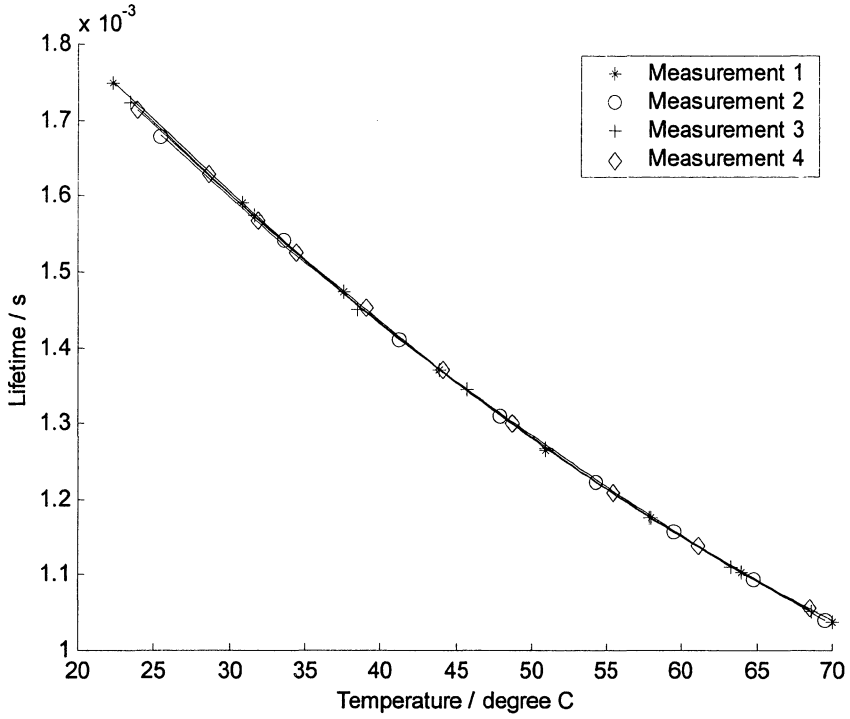

Figure 35. The lifetime as a function of temperature for Cr:YAG.
The reproducibility is almost as good as for alexandrite

The curve fitted to the four measurements and the standard deviation, 2.7 x 10^{-6} s, can be seen in Figure 36. The relative standard deviation was determined to 0.20 %. Only a part of the curve is shown in the graph. The temperature sensitivity of Cr:YAG is approximately ± 0.25 °C.

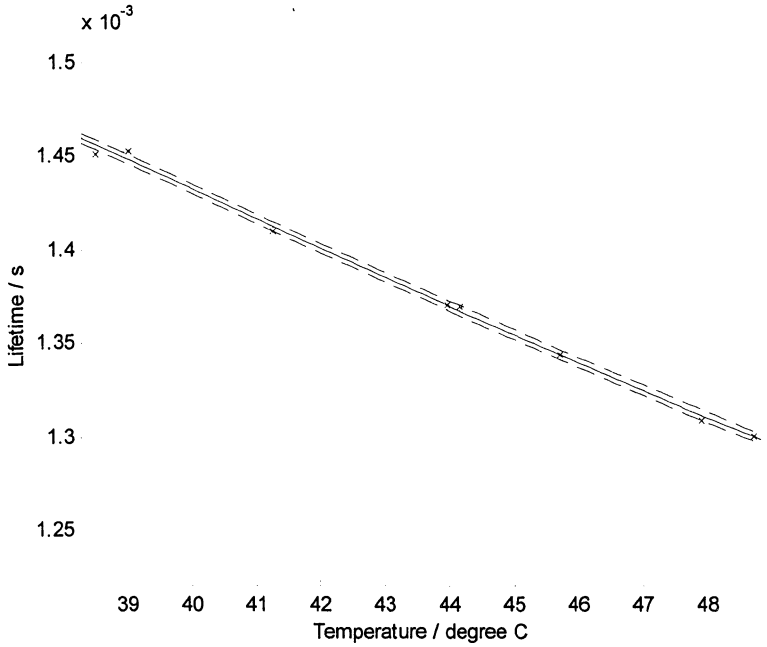

Figure 36. The fitted curve to the four measurements for Cr:YAG, solid line, and the standard deviation, dashed line

In Figure 37 the results from the fluorescence intensity ratioing method for the four measurements that were done for Cr:YAG can be seen. The graph again indicates a good reproducibility.

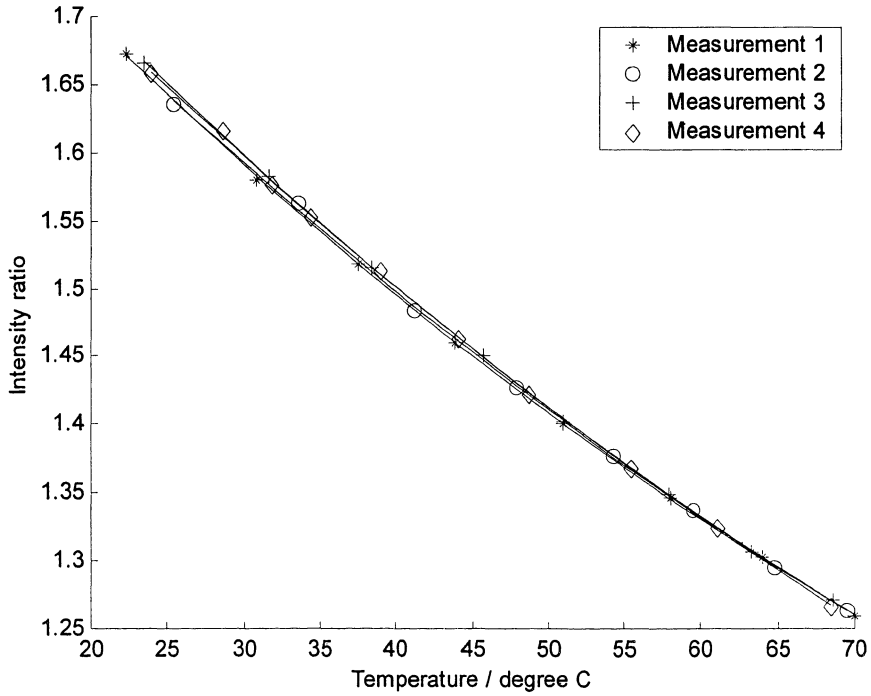

Figure 37. Fluorescence intensity ratio as a function of temperature for Cr:YAG

4.1.3 Cr:LiSAF

In Figure 38 the lifetime for Cr:LiSAF is plotted as a function of temperature. Four different measurements are included and the graph shows the reproducibility.

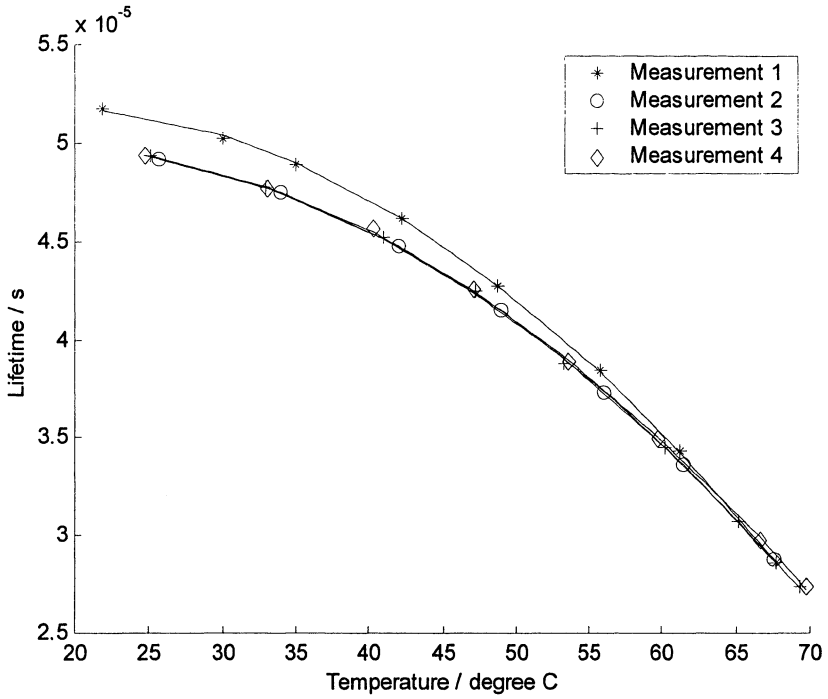

Figure 38. The lifetime as a function of temperature for Cr:LiSAF.
It also shows the reproducibility

The curve fitted to the last three measurements and the standard deviation, 1.4 x 10^{-7} s, are included in Figure 39. The first measurement was omitted due to its deviation from the others. The relative standard deviation was 0.35 %. Only a part of the curve is shown in the graph. The temperature sensitivity for Cr:LiSAF is estimated to ± 0.3 °C.

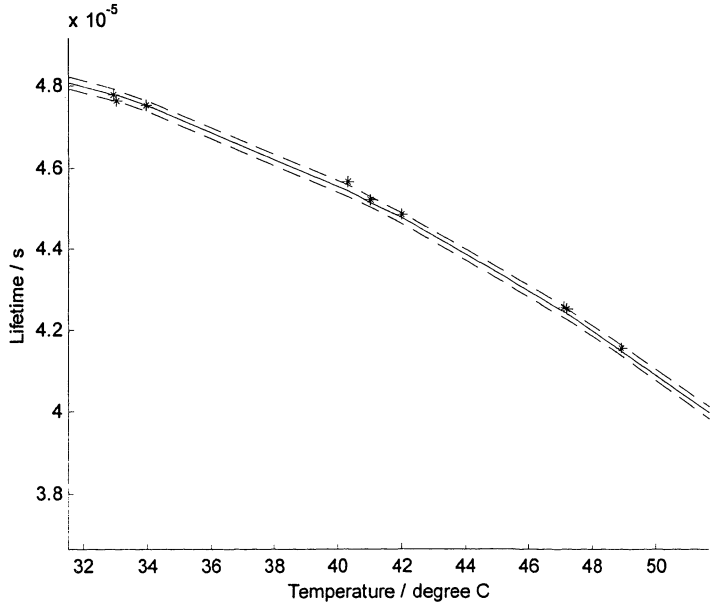

Figure 39. The fitted curve to the last three measurements for Cr:LiSAF, solid line, and the standard deviation, dashed line

4.2 Measurements on crystal attached to fibre tip

Continued experiments were performed on alexandrite and Cr:LiSAF with the fluorescence lifetime method. The crystals were glued onto fibre tips. Two different glues were used to see if the glue effected the fluorescence.

4.2.1 Alexandrite

The fluorescence spectra from alexandrite with the two different glues were compared and no significant difference in the results was obtained. In Figure 40 the fluorescence lifetime as a function of temperature is seen, for the crystal glued with Norland Optical Adhesive 68, Norland Products, together with the standard deviation, 4.0 x 10^{-7} s. The relative standard deviation was determined to 0.20 %. Only a part of the temperature interval is shown for clarity. The temperature sensitivity was estimated to ± 0.2 °C.

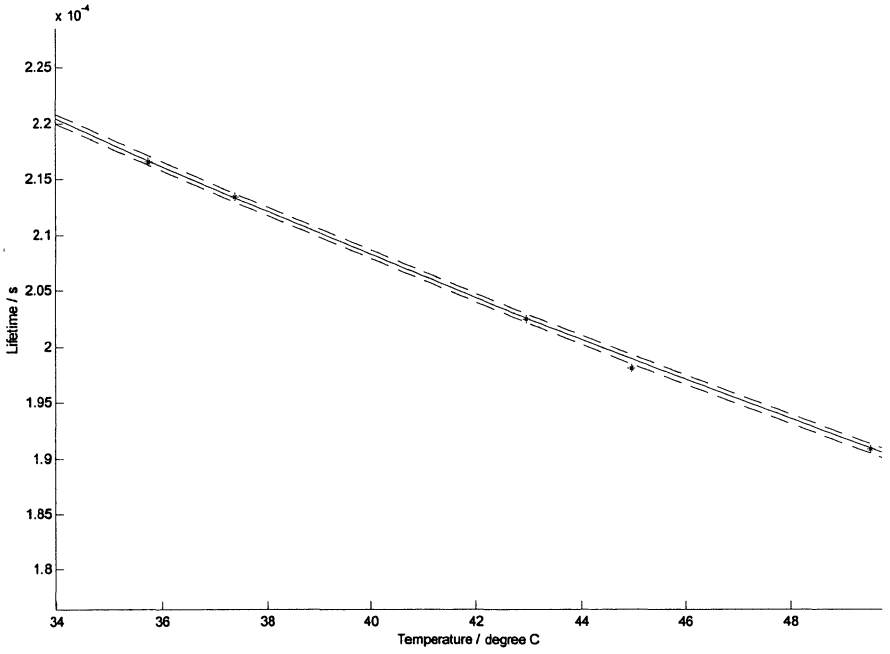

Figure 40. The lifetime as a function of temperature for alexandrite glued to fibre, solid line, and standard deviation, dashed line

4.2.2 Cr:LiSAF

No difference could be seen in the fluorescence spectra from the Cr:LiSAF with the two different glues. In Figure 41 the fluorescence lifetime as a function of temperature is seen, for the Cr:LiSAF glued with Norland Optical Adhesive 68, Norland Products. The standard deviation, 1.3 x 10^{-7} s, is also seen in the figure. The relative standard deviation was 0.24 %. Only a part of the temperature interval is shown for clarity. The temperature sensitivity for Cr:LiSAF was estimated to ± 0.3 °C.

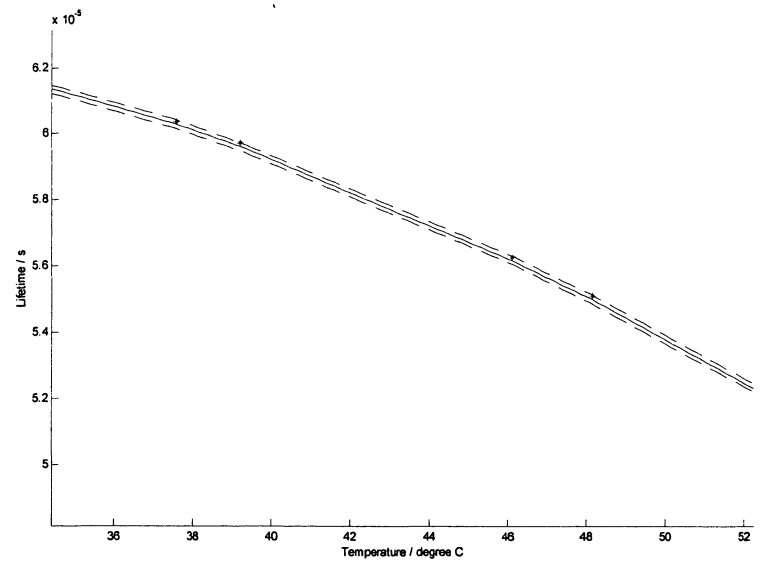

Figure 41. The lifetime as a function of temperature for Cr:LiSAF glued to fibre, solid line, and standard deviation, dashed line

4.3 Fibre measurements with PDT laser

The calibration curve for Cr:LiSAF can be seen in Figure 42. The lifetime is plotted versus the temperature, the standard deviation, 3.2 x 10^{-7} s, can also be seen. The relative standard deviation was determined to 0.85 %. The corresponding temperature accuracy is approximately ± 0.5 °C.

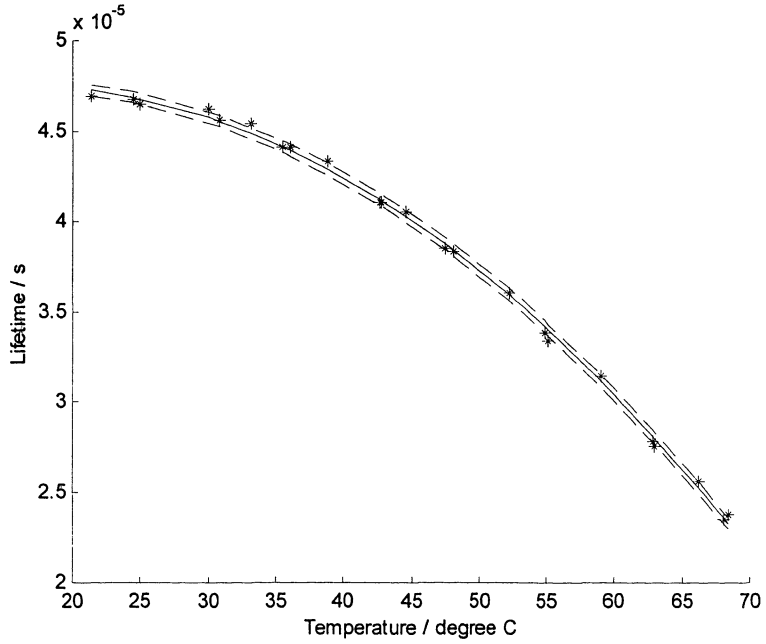

Figure 42. The calibration curve, solid line, for Cr:LiSAF and standard deviation, dashed line

The spectra recorded with the OMA system show how the Cr:LiSAF crystal fluoresces when excited at 405 nm (Figure 43). The tissue autofluorescence from the skin recorded by the same fibre is illustrated in Figure 44. The fluorescence from the fibre is subtracted from both spectra.

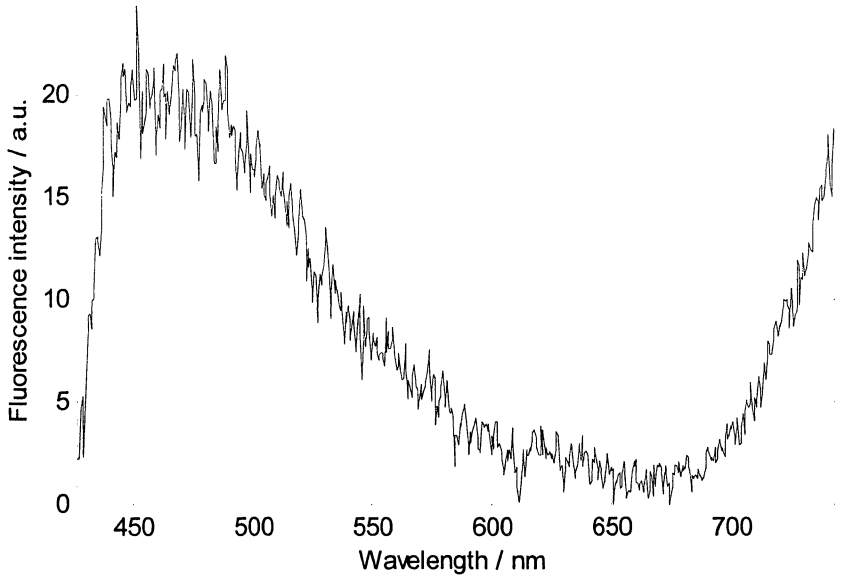

Figure 43. The fluorescence from Cr:LiSAF when excited with 405 nm

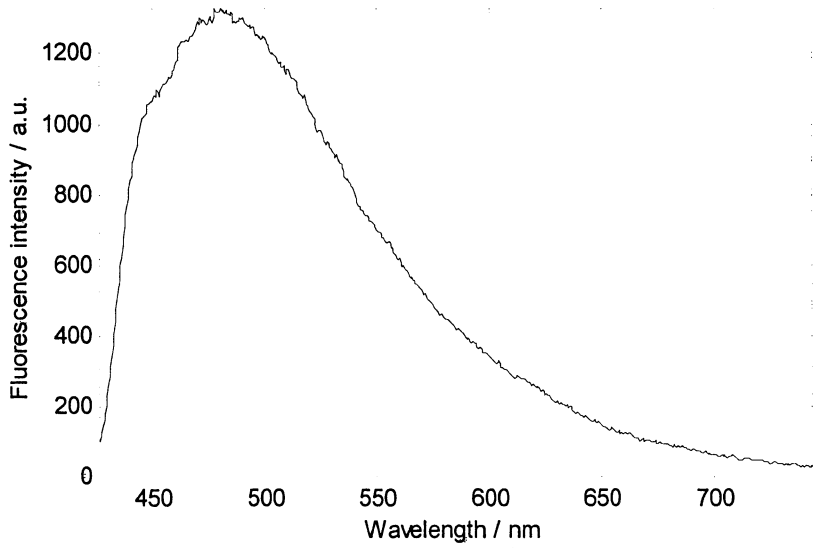

Figure 44. Tissue autofluorescence, excitation wavelength 405 nm

Figure 45 shows the autofluorescence taken with the fibre with the glued crystal when excited at 405 nm. The crystal fluorescence is subtracted.

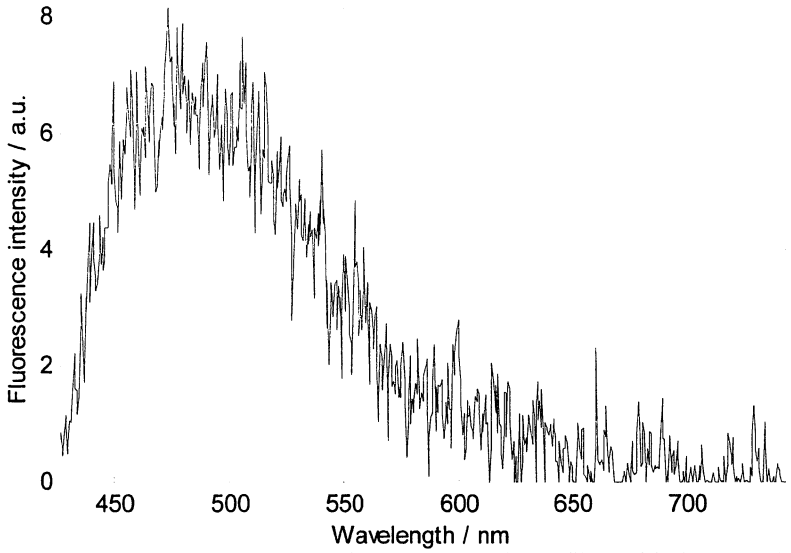

Figure 45. Autofluorescence detected through the fibre with the crystal

4.4 Test measurements on pork chop

Figure 46 shows the calibration curve together with the measurements on the pork chop.

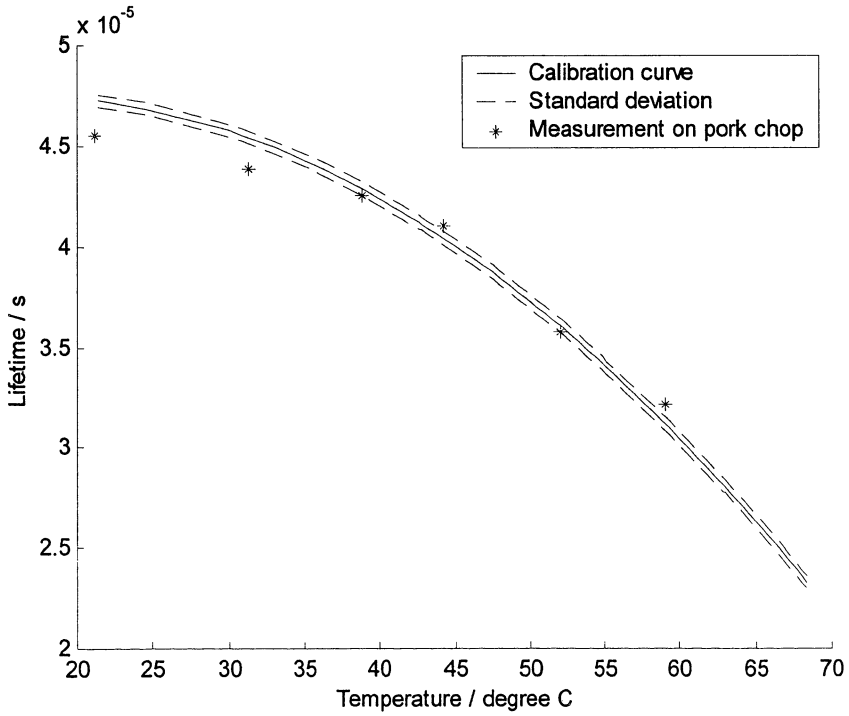

Figure 46. Calibration curve, solid line, and standard deviation, dashed line, together with the measurements on pork chop, *

One spectrum taken with the diode laser fluorosensor at 21 °C can be seen in Figure 47. The exciting laser light is at 396 nm, and the continuum between 450 – 650 nm is a superposition of tissue autofluorescence from the pork chop, fibre fluorescence and fluorescence from Cr:LiSAF. The fluorescence from Cr:LiSAF is also seen between 700 – 1000 nm. The narrow peak close to 800 nm is due to second order diffraction of the laser light on the grating.

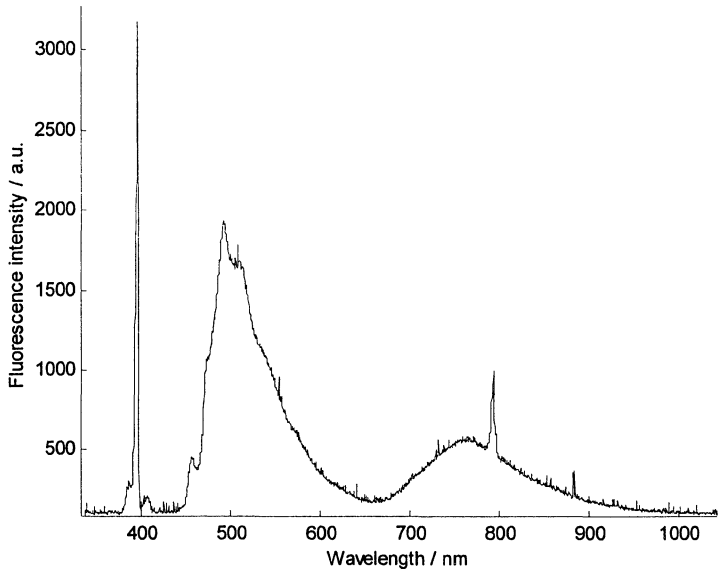

Figure 47. Fluorescence spectrum from the pork chop, the fibre and Cr:LiSAF recorded by the diode laser fluorosensor

4.5 Simulation of an IPDT treatment

In Table 4 the different values from the simulaton of the IPDT treatment are listed.

Table 4. Values from the simulation

Time / min	Thermistor 1 / °C	Thermistor 2 / °C	Fluorescence lifetime / μs
0	19.0	18.8	47.8
15	19.8	19.5	46.7

The photos taken with the IR camera before (Figure 48) and after (Figure 49) the treatment show the temperature distribution in the pork chop. The fibre tip with the crystal is inside the circle. The checked plate in the figures is used as a ruler and a reference because its known emissivity, e = 1.

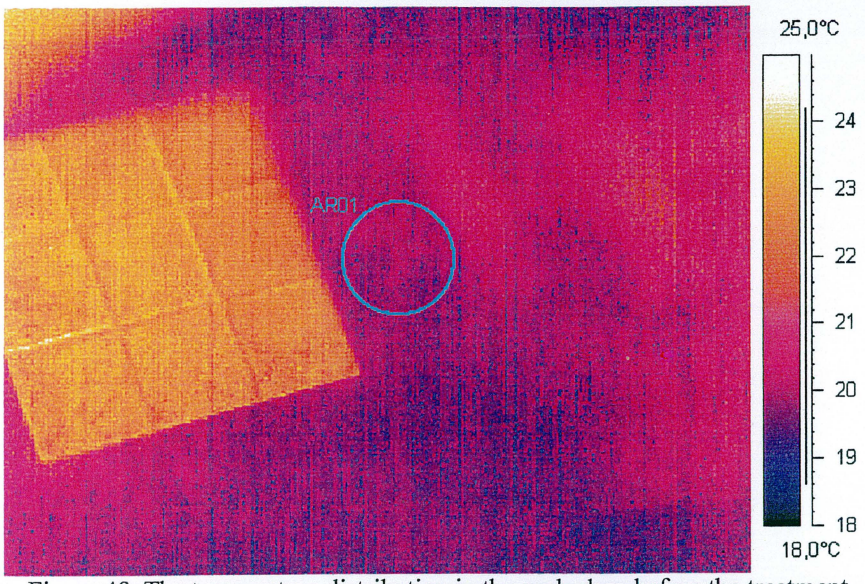

Figure 48. The temperature distribution in the pork chop before the treatment, inside the circle the maximum temperature is 20.9 °C

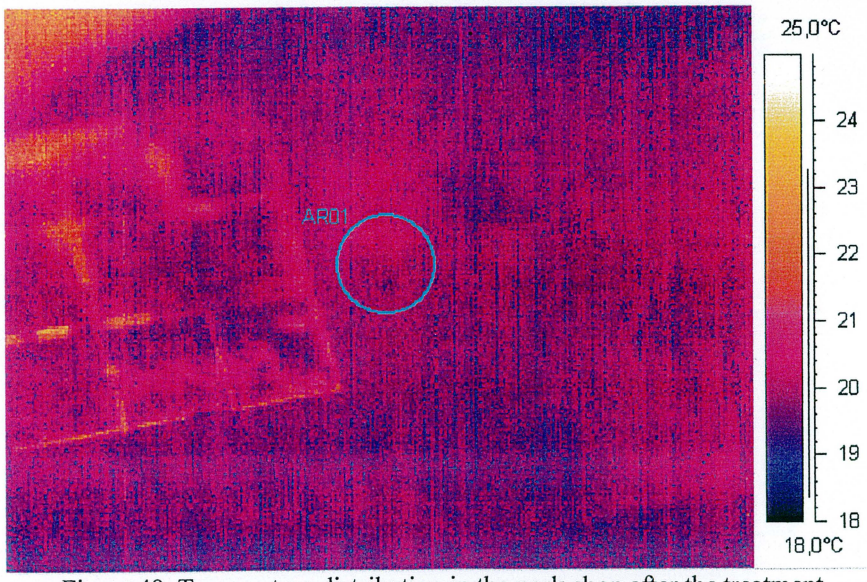

Figure 49. Temperature distribution in the pork chop after the treatment, inside the circle the maximum temperature is 21.0 °C

5 Discussion

5.1 Initial experiments on three Cr^{3+}-doped crystals

5.1.1 Alexandrite

The four series of measurements made on a piece of alexandrite (Figure 32) with the lifetime method indicates a good reproducibility, since they all ended up at the same curve. This made it easy to fit a curve to all the measurements and the standard deviation was relatively small. Our data was compared to another group's results, Grattan *et al.* This group fitted the equation below to their data, to get an estimation of τ_s, α and ΔE.

$$\tau = \tau_s \frac{1 + 3e^{-\Delta E / kT}}{1 + \alpha e^{-\Delta E / kT} + \beta e^{-(\Delta E_q + \Delta E)/kT}}$$

For temperatures below 600 K the thermal quenching is negligable, thus the term $\beta e^{-(\Delta E_q + \Delta E)/kT}$ can be excluded in the equation. Grattan *et al.* evaluated the fitted parameters to; τ_s = 1.17 ms, lnα = 5.40 and ΔE = 857 cm^{-1}.[10] In Figure 50 our data is compared to the values retrieved by Grattan *et al.* If the equation above is adjusted to our data, we recieve the parameters; τ_s = 1.16 ms, lnα = 5.44 and ΔE = 850 cm^{-1}.

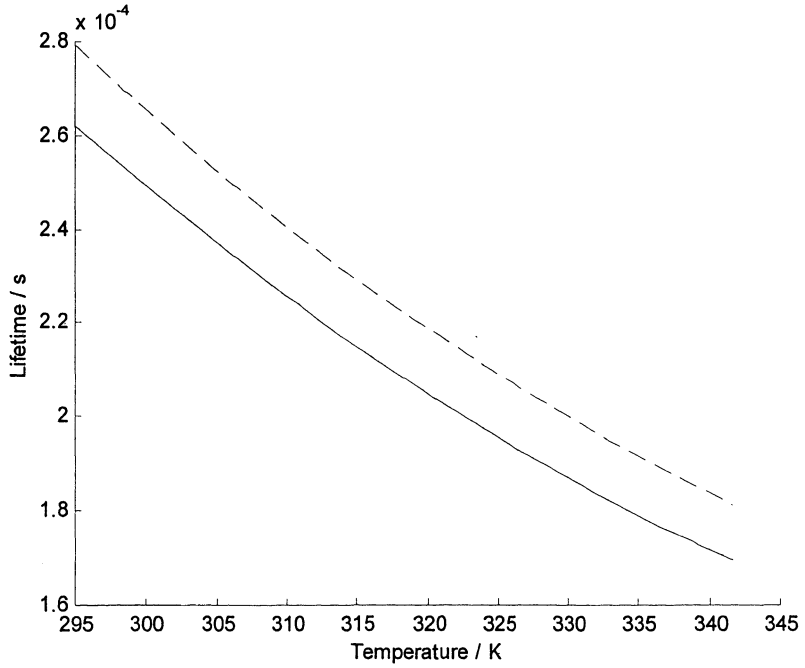

Figure 50. Lifetime as a function of temperature for alexandrite, our results (solid line) and Grattan *et al.* results (dashed line)

As can be seen in the figure our results do not match the one from the literature. There can be several explanations for this. First of all we do not know if their results are correct, spectroscopic data mentioned by Grattan *et al.* are τ_s = 1.32 ms and ΔE = 807.5 cm^{-1}, but no values on lnα have been reported.[10] It is also possible that our thermistors are not properly calibrated. The crystal can also be warmer than the two thermistors, when they are not in the exact same position as the crystal. Our equipment is also very sensitive to

the amount of fluorescence intensity. If the intensity is too low, the system becomes unstable, thus showing a too short lifetime. It is important that no laser light is detected together with the fluorescence light, since this may shorten the measured lifetime. Even a very small amount of laser light can ruin the measurement, therefore it is important to choose optical filters that efficiently block the laser light.

Even though our lifetimes are not identical with the results from Grattan *et al.*, they show the same slope and are in the same range. This gives the possibility to measure the temperature with the lifetime method with our equipment.

In the fluorescence ratioing method the reproducibility was not so good compared to the lifetime method. Since the series of measurements differed, no curve was fitted to them and no standard deviation was calculated. The method can perhaps be improved if the choice of the integrated areas is optimised.

5.1.2 Cr:YAG

The lifetime measurements made with a Cr:YAG crystal show a good reproducibility (Figure 35), and there were no difficulties when fitting a curve to the measurements. The standard deviation was satisfyingly small. A comparison of our results with Zhang *et al.*[12] was done in the same way as for alexandrite in section 5.1.1. This can be seen in Figure 51.

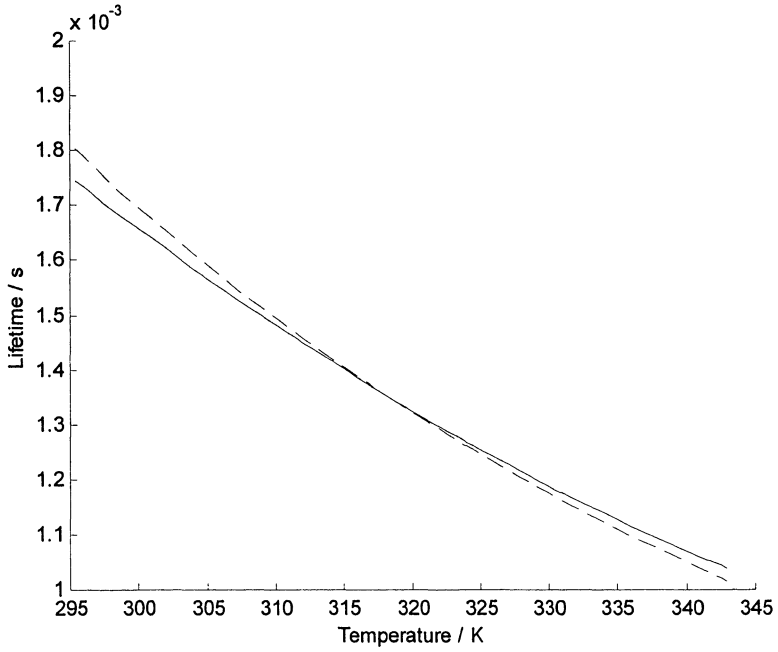

Figure 51. The lifetime as a function of temperature for Cr:YAG, our values (solid line) and the values of Zhang *et al.* (dashed line)

Zhang *et al.* recieved the fitted values τ_s = 7.41 ms, lnα = 6.35 and ΔE = 1066 cm^{-1}.[12] There were no spectroscopic values to compare with. Our results are quite close to the results of Zhang *et al.*, but the two curves have slightly different slopes. An explanation to this can be that our Cr:YAG crystal was doped by both Fe, 4 ppm, and Co, 20 ppm, to quench the fluorescence. When adjusting the equation above to our data, we recieved the

same values of the parameters as Zhang *et al.* It was impossible to recieve the same slope as Zhang *et al.*

The reproducibility for the fluorescence intensity ratioing method for Cr:YAG was quite good, but not as good as for the lifetime method. The fluorescence spectrum was more complicated because of the Fe and Co effects, but even though it would be possible to choose this method.

5.1.3 Cr:LiSAF

In Figure 38 one could see that the first measurement for Cr:LiSAF was not in accordance with the other three. We have no explanation to this, but since the other three measurements were so similar, the first measurement was excluded when fitting a curve to the data. The standard deviation for the last three measurements was relatively small. As for the other two crystals a comparsion was made with results from Grattan *et al.* Since Cr:LiSAF is a crystal with a low crystal field strength, a different equation was used by Grattan.

$$\tau = \frac{\tau_i}{1 + \beta e^{-\Delta E_q / kT}}$$

The values of the parameters, when fitted to their data, were; $\ln\beta = 18.89$, $\tau_i = 62.25$ μs and $\Delta E_q = 4557$ cm^{-1}.[10] A comparision between our data and the ones from Grattan *et al.* can be seen in Figure 52. When we adjusted the equation above to our data, the values of the parameters were; $\ln\beta = 19.0$, $\tau_i = 52.5$ μs and $\Delta E_q = 4550$ cm^{-1}.

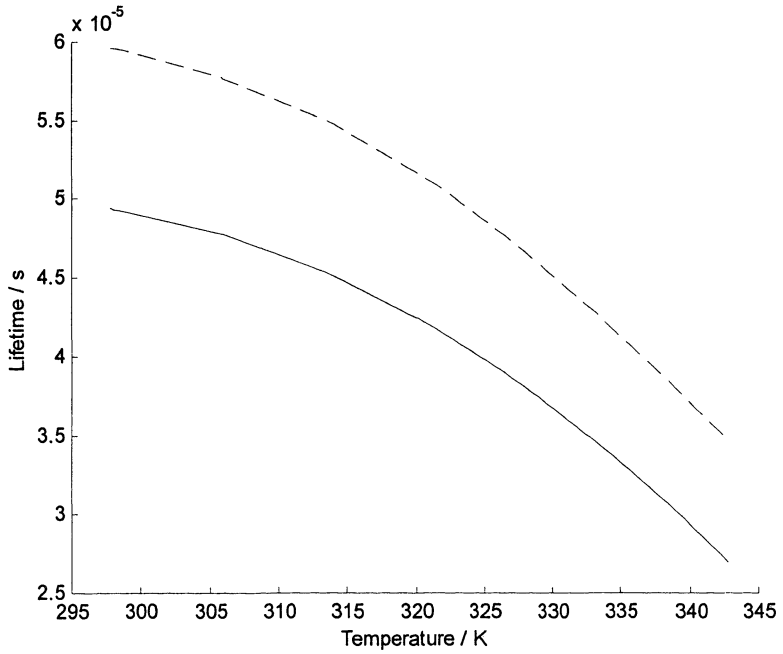

Figure 52. The lifetime as a function of temperature for Cr:LiSAF, our data (solid line) and Grattan's results (dashed line)

Our results showed a shorter lifetime than the results of Grattan, but the curves had the same shape. The causes to this can be the same as the ones discussed in section 5.1.1.

Since the fluorescence intensity method was not applicable to Cr:LiSAF, the lifetime method was the only choice. This is not a drawback since the lifetime method gives good results.

5.1.4 Comparison between the three crystals and the two methods

When comparing the three crystals they all have a relatively high accuracy, within the required limit ± 0.5 °C. Cr:LiSAF has not got a so high slope between 20 – 25 °C as the other two crystals. But since the temperature during an IPDT treatment is over 30 °C this has less relevance. All the crystals have longer lifetimes, μs – ms, than PpIX, which has a lifetime in the nanosecond region. This makes it possible to separate the fluorescence from the crystals from the fluorescence from PpIX in time.

For further experiments Cr:YAG was not selected because of the strong fluorescence in the red region, making it impossible to detect other fluorophores, for example PpIX, when monitoring the fluorescence spectrum during an IPDT treatment.

The two methods have different advantages. The fluorescence intensity method requires less complicated equipment and could more easily be incorporated with the IPDT system. One disadvantage is that the fluorescence from other fluorophores can complicate the ratioing, if they fluoresce in the same region as the crystal. The fibre fluorescence can also interfere with the measurements. The method seems more inaccurate than the lifetime method, but if the requirement of accuracy is not so high, this should not matter. The lifetime method needs more advanced equipment, but is not as sensitive to tissue fluorescence, since both the wavelength range and lifetimes are quite different.

When comparing the two methods the lifetime method seemed more suitable and was therefore chosen in following experiments. Since it is not possible to use the fluorescence intensity method for Cr:LiSAF we had to measure the fluorescence lifetime.

The cost for the different crystals varies quite a lot. Cr:LiSAF is comparably expensive, but since so small amounts of the crystal are needed for each fibre this should not be a deciding factor.

5.2 Measurements on crystal attached to fibre tip

When comparing the results from our previous measurements on a whole crystal with the ones recieved when a piece of the crystal was glued to the fibre tip, one can see that there is a difference in measured lifetimes. This can be due to the reasons already mentioned in section 5.1.1.

Even though the type of glue did not have any effect on the fluorescence spectrum, the method to glue the crystal to the fibre is not a good choice for this purpose. This is due to the difficulty to place the crystal in a position on the fibre tip so that the detected fluorescence intensity is as high as possible. As stated before only a little decrease in the fluorescence can effect the fluorescence lifetime measurements. Another problem is that the glue does not attach so hard to the fibre, resulting in that the crystal very easily falls off when subjected to mechanical stress. The amount of glue used can also effect the results, when a lot of glue between the fibre and crystal can decrease the fluorescence

intensity as well as the detected light. A better alternative would be to dope the fibre tip with the crystal.

Due to the fact that alexandrite has a very high absorption at 405 nm and that Cr:LiSAF absorbs relatively little around 405 nm, Cr:LiSAF is prefeered. The Cr:LiSAF fluorescence spectrum has no sharp peaks in the red wavelength region. This makes it easy to separate the peaks of the PpIX fluorescence from the fluorescence originating from the crystal.

5.3 Fibre measurements with PDT laser

The calibration curve was done with a different fibre than the one used in section 5.2, this explains why the calibration curve has different lifetimes. This measurement did not give the same accuracy as our previous results, but it still fulfills the requirements. An explanation to this can be that the crystal is further away from the fibre tip, resulting in a decrease in fluorescence intensity. This indicates that each fibre made in this way needs to be treated individually and a calibration curve, versus known temperatures, has to be made for each fibre. The most important thing is to know which temperature a specific lifetime corresponds to, and if this is in agreement with theoretical data is less important.

When Cr:LiSAF is excited with light at 405 nm (Figure 43) it fluoresces very little in the region 600 – 700 nm. This prevents the PpIX fluorescence from being drowned by crystal fluorescence. When using a fibre with a crystal glued to the tip one can detect the autofluorescence through this fibre, see Figure 45. This is important for the future development of the IPDT system. The autofluorescence has to be detected to be able to monitor the treatment.

5.4 Test measurements on pork chop

In Figure 46 one can see that the lifetime measurements on pork chop give a shorter fluorescence lifetime than expected for lower temperatures. The results for higher temperatures follow the calibration curve better. This can be interpreted as, for lower temperatures the crystal is also heated by the laser light, but at higher temperatures this heating process becomes negligible.

Spectra were also recorded by the diode fluorosensor, Figure 47. This was done to see if the system could detect the fluorescence spectrum from the crystal as well as the fluorescence spectrum from the pork chop. Since the autofluorescence and the fluorescence from the crystal overlap in the region between 450 – 600 nm, it is difficult to detect the autofluorescence at the same time as the fluorescence from the crystal, without effecting each other. Therefore it seems that the fluorescence intensity ratioing method will be difficult to achieve, since it is important to measure the autofluorescence correctly. Little fluorescence from the crystal was observed between 600 and 700 nm, making it possible to detect PpIX fluorescence. Above 700 nm only fluorescence from the crystal was detected.

5.5 Simulation of an IPDT treatment

The thermistors' results from the simulation of an IPDT treatment show an increase in temperature of 19.0 °C to 19.8 °C. The fluorescence lifetime decreases from 47.8 μs to 46.7 μs. How many degrees in °C this corresponds to is difficult to say, since the calibration curve ends at 20 °C and is very flat in this region. An extrapolation of the curves suggests an increase of less than 5 °C. The photos taken with the IR camera show only a very small increase in temperature.

All the three methods show an increase in temperature, but a very low one. It is a good result that there is a very small increase in temperature during an IPDT treatment, since IPDT is not a thermally therapeutic treatment. The output power from the fibre is only a third of the actual power during an IPDT treatment but this should not alter the results drastically, as long there is no coagulation. If coagulation occurs in an IPDT treatment the temperature at the fibre tip is assumed to increase dramatically due to increased absorption of the therapeutic light and loss of cooling perfusion.

5.6 Further research and development

As already mentioned there are lots of improvements to the attachment of the crystal at the distal end of the fibre to be done. The best alternative would probably be to dope the fibre tip by the crystal. This would protect both the patients from the crystal and the crystal from the outer environment. This would also increase the mechanical durability and make it possible to sterilize the fibre. The aim is to have a power output of approximately 100 mW from the fibre tip. To accomplish this the crystal can not be glued to the fibre tip, since the crystal becomes too large and the glue will back scatter the light back in to the fibre.

Another improvement would be to change the chopper wheel for an acousto-optic modulator, AOM, to be able to have a stable frequency during the measurements. The chopper wheel shows difficulties to keep the same frequency and drifts away. With an AOM the reference signal to the lock-in amplifier would be more accurate.

The filter box in our set up turned out to be difficult to align and the beam splitter was not optimised for the wavelenghts used. This resulted in high intensity losses. This could be improved since more suitable solutions are commercially available.

The fluorescence intensity ratioing method could be an alternative to measure the temperature. Some improvements have to be made and the chosen crystal needs to have visible sharp peaks and not just a broad band, otherwise it becomes impossible to calculate a ratio. It is possible to use this method if the requirements of the accuracy are not very high. Sudden changes could, if something goes wrong, be detectable and this is the main purpose, so the treatment can be interrupted. The method can effect the measurements of the tissue autofluorescence.

In the future the hope is to incorporate an OMA system with the IPDT system. This would make it possible to study the tissue autofluorescence and the fluorescence from PpIX during a treatment. The OMA system will then excite at 405 nm. It would also be desirable to measure the temperature with this improved system. Both the fluorescence lifetime and the fluorescence intensity ratioing method could be used in the system to

measure the temperature. Even though the fluorescence lifetime method gives a better accuracy, these measurements might be more difficult to incorporate in the system.
It is also possible that crystals, other than Cr^{3+}-doped crystals, can be used for this task. One alternative would be to excite with 405 nm instead. In this case the temperature can only be measured at the same time as the tissue autofluorescence. It is important that the chosen crystal does not fluoresce at the same wavelengths as the fluorophores, and that it does not absorb too much at 405 nm, effecting the intensity of the autofluorescence.

There could be some possible candidates among the rare-earth metals for exciting with light at 405 nm, for example Sm^{3+}, Eu^{3+}, Tb^{3+}, Dy^{3+} and Ho^{3+}. Some of these may not be suitable for medical application due to toxic effects. Further studies need to be done.

6 Conclusions

We have established that it is possible to measure the temperature through optical fibres by studying the fluorescence from Cr^{3+}-doped crystals. These crystals show a strong temperature dependent fluorescence. An accuracy better than ± 0.5 °C was accomplished.

In this work Cr:LiSAF seemed to be the crystal with the most suitable properties, but it would not be impossible to use alexandrite instead. The main disadvantage for alexandrite is the relatively high absorption at 405 nm, which would effect the study fluorescence of the fluorophores.

Two different methods were evaluated, one measures the lifetime of the fluorescence and one is based on fluorescence intensity ratioing. The fluorescence lifetime method gives a higher accuracy than the fluorescence intensity ratioing method, but requires more advanced equipment. Both methods need further developement, before they can be incorporated in the IPDT system.

After initial experiments in air, some measurements were performed on pork chop as a tissue phantom to see if the method could be used in tissue experiments. The result showed that this seemed possible.

7 Acknowledgements

First of all we would like to thank our supervisor Stefan Andersson-Engels for all his help with the project and his patience with us. He has been very supportive and optimistic during the time we have been in the Medical Group.

Thomas Johansson is also to be thanked for all the valuable help with the electronic equipment down in the dark laboratory.

Special thanks to the rest of the members of the Medical Group for all their assistance and nice company.

We would also like to thank everyone at the Division of Atomic Physics who has given us a helping hand.

References

1. S. Svanberg, *Atomic and Molecular Spectroscopy – Basic Aspects and Practical Applications* , (Springer Verlag, Heidelberg, Germany, 2001).

2. C. af Klinteberg, On the use of light for the characterization and treatment of malignant tumours, Dissertation thesis, Lund Institute of Technology, Lund, Sweden (1999).

3. T. Johansson, M. Soto Thompson, M. Stenberg, C. af Klinteberg, S. Andersson-Engels, S. Svanberg and K. Svanberg, Feasibility study of a novel system for combined light dosimetry and interstitial photodynamic treatment of massive tumors, *Applied Optics,* (2001). (In press).

4. C. Eker, Optical characterization of tissue for medical diagnostics, Dissertation thesis, Lund Institute of Technology, Lund, Sweden (1999).

5. I. Wang, Photodynamic therapy and laser-based diagnostic studies of malignant tumours, Dissertation thesis, Lund University, Lund, Sweden (1999).

6. Q. Peng, T. Warloe, K. Berg, J. Moan, M. Kongshaug, K.-E. Giercksky and J.M. Nesland, 5-aminolevulinic acid-based photodynamic therapy: Clinical research and future challenges, *Cancer* **79**, 2282-2308 (1997).

7. H. Schneckenburger, K. König, K. Kunzi-Rapp, C. Westphal-Frösch and A. Ruck, Time-resolved in-vivo fluorescence of photosensitizing porphyrins, *J. Photochem. Photobiol. B* **21**, 143-147 (1993).

8. B.G. Potter Jr and M.B. Sinclair, Photosensitive and rare-earth doped ceramics for optical sensing: a review, *Journal of Electroceramics* 295-308 (1998).

9. A.A. Kaminskii, *Laser crystals their physics and properties*, (Springer Verlag, Heidelberg, Germany, 1990).

10. K.T.V. Grattan and Z.Y. Zhang, *Fiber optic fluorescence thermometry*, (Chapman & Hall, London, 1995).

11. B. Henderson and G.F. Imbusch, *Optical spectroscopy of inorganic solids*, (Oxford university press, USA , 1989).

12. Z.Y. Zhang, K.T.V. Grattan, A.W. Palmer, V. Fernicola and L. Crovini, Temperature dependence of the YAG:Cr^{3+} fluorescence lifetime over the range 77 to 900 K, *Physical Review B* **51**, 2656-2660 (1995).

13. R.C. Powell, L. Xi, X. Gang, G.J. Quarles and J.C. Walling, Spectroscopic properties of alexandrite crystals, *Physical Review B* **32**, 2788-2797 (1985).

14. O. Svelto, *Principles of Lasers*, (Plenum, 1998).

15. V. Fernicola and L. Crovini, Cr:YAG fluorescence-decay for optical-fiber temperature sensors, *SPIE Fiber optic and laser sensors XI* **2070**, 472-477 (1993).

16. Z. Zhang, K.T.V. Grattan and A.W. Palmer, Sensitive fiber optic thermometer using Cr:LiSAF fluorescence for biomedical sensing applications, *8:th optical fiber sensors conference*, Monterey, California, USA, 1992.

17. T. Sun, K.T.V. Grattan, Z.Y. Zhang, A.W. Palmer, S.F. Collins, G.W. Baxter and S.A. Wade, Fluorescence-based measurement schemes using doped fiber: theoretical analysis and experimental validation, in *Nonlinear Optics '98: Materials, fundamentals and applications topical meeting, 1998.*, Proc. IEEE 107-109 (1998).

18. L. Armstrong and S. Ferneuille, Theoretical analysis of the phase shift measurement of lifetimes using monochromatic light, *Journal of Physics B* **8**, 546 (1975).

19. C. af Klinteberg, M. Andreasson, O. Sandström, S. Andersson-Engels and S. Svanberg, Compact medical fluorosensor for minimally invasive tissue characterisation, Manuscript in preparation (2001).

20. C. Sturesson, Medical laser-induced thermotherapy - models and applications, Dissertation thesis, Lund Institute of Technology, Lund, Sweden (1998).

21. U. Gustafsson, S. Pålsson and S. Svanberg, Compact fibre-optic fluorosensor using a continuous wave violet diode laser and an integrated spectrometer, *Rev. Sci. Instrum.* **71**, 3004-3006 (2000).